INL/EXT-17-41653

RELAP-7 Closure Correlations

L. Zou, R.A. Berry, R.C. Martineau, D. Andrs, H. Zhang, J.E. Hansel, J.P. Sharpe
Idaho National Laboratories

R.C. Johns
Los Alamos National Laboratory

April 2017

U.S. Department of Energy
Office of Nuclear Energy

INL REPORT

INL/EXT-17-41653
Unlimited Release
April 2017

RELAP-7 Closure Correlations

Prepared by
Idaho National Laboratory
Idaho Falls, Idaho 83415

The Idaho National Laboratory is a multiprogram laboratory operated by
Battelle Energy Alliance for the United States Department of Energy
under DOE Idaho Operations Office. Contract DE-AC07-05ID14517.

Issued by the Idaho National Laboratory, operated for the United States Department of Energy by Battelle Energy Alliance.

Printed in the United States of America. This report has been reproduced directly from the best available copy.

INL/EXT-17-41653
Unlimited Release
April 2017

RELAP-7 Closure Correlations

L. Zou, R.A. Berry, R.C. Martineau, D. Andrs, H. Zhang, J.E. Hansel, J.P. Sharpe

Idaho National Laboratory

R.C. Johns

Los Alamos National Laboratory

Contents

Summary 8
1 Introduction 9
2 Seven-Equation Two-Phase Flow Model 10
3 Wall Drag 12
3.1 Single-Phase Flow 12
3.2 Two-Phase Flow: Pre-CHF Flow Regimes 13
3.2.1 Bubbly/Slug Flow Regime 13
3.2.2 Annular/Mist Flow Regime 14
3.2.3 Transition between Bubbly/Slug and Annular/Mist Flow Regimes . 15
3.2.4 Horizontal Stratified Flow 15
3.2.5 Transition between Horizontal Stratified and Non-Stratified Flow . . 17
3.3 Two-Phase Flow: Post-CHF Flow Regimes 18
3.3.1 Inverted Annular Flow 18
3.3.2 Dispersed Flow 19
3.3.3 Transition between Inverted Annular and Dispersed Flow 20
4 Interfacial Drag 21
4.1 Pre-CHF Flow Regimes 21
4.1.1 Bubbly/Slug Flow 21
4.1.1.1 Pipe Geometry 22
4.1.1.2 Rod Bundle Geometry 23
4.1.2 Annular/Mist Flow 23
4.1.3 Mixing of Bubbly/Slug and Annular/Mist Flows 26
4.1.4 Horizontal Stratified Flow 26
4.1.5 Transition between Horizontal Stratified and Non-Stratified Flow . . 27
4.2 Post-CHF Flow Regimes 27
4.2.1 Inverted Annular Flow 27
4.2.2 Inverted Slug Flow 29
4.2.3 Dispersed Flow 29
4.2.4 Transition between Inverted Annular and Inverted Slug Flow Regimes 31
4.2.5 Transition between Inverted Slug and Dispersed Flow Regimes . . . 31
5 Interfacial Heat Transfer 32
5.1 Pre-CHF Flow Regimes 32
5.1.1 Bubbly Flow 32
5.1.2 Cap Bubble/Slug Flow 34
5.1.3 Correction for Subcooled Boiling 36
5.1.4 Annular/Mist Flow 36
5.1.5 Transition between Bubbly/Slug and Annular/Mist Flow 39
5.1.6 Horizontal Stratified Flow 39
5.1.7 Transition between Stratified and Non-Stratified Flow 40
5.2 Post-CHF Flow Regimes 40

5.2.1 Inverted Annular Flow 41
5.2.2 Inverted Slug and Dispersed Flow 41
5.2.3 Interpolation Region 43
6 Wall Heat Transfer 44
6.1 Pre-CHF Wall Heat Transfer 44
6.1.1 Single-Phase Liquid Flow 44
6.1.1.1 Tube Geometry 46
6.1.1.2 Rod Bundle Geometry 47
6.1.2 Two-Phase Forced Convection 48
6.1.3 Film Condensation 48
6.1.4 Transition between Two-Phase Forced Convection and Film Condensation 49
6.1.5 Wall Boiling Heat Transfer 49
6.1.5.1 Onset of Nucleate Boiling 50
6.1.5.2 Nucleate Boiling Heat Transfer 50
6.2 Post-CHF Wall Heat Transfer 51
6.2.1 Inverted Annular Film Boiling 51
6.2.2 Dispersed Flow Film Boiling 53
6.2.2.1 Wall-to-Vapor-Phase Convective Heat Transfer 53
6.2.2.2 Wall-to-Liquid/Vapor-Phase Radiation Heat Transfer . . . 55
6.2.2.3 Summary 57
6.2.3 Inverted Slug Film Boiling 57
6.2.4 Transition Boiling 58
References 60

Figures

1 Schematic drawing of the horizontal stratified flow. 16
2 Post-CHF flow regime map [3]. 28
3 Flow regime map in vertical pipes under the pre-CHF conditions, for interfacial heat transfer [3]. 33
4 Logic to determine pre-CHF wall heat transfer mode following TRACE code [3]. 45
5 Logic to determine post-CHF wall heat transfer mode following TRACE code [3]. 52

Summary

The RELAP-7 code is the next generation nuclear reactor system safety analysis code being developed at the Idaho National Laboratory (INL). The code is based on the INL's modern scientific software development framework, MOOSE (Multi-Physics Object Oriented Simulation Environment). The overall design goal of RELAP-7 is to take advantage of the previous thirty years of advancements in computer architecture, software design, numerical integration methods, and physical models. The end result will be a reactor systems analysis capability that retains and improves upon RELAP5's and TRACE's capabilities and extends their analysis capabilities for all reactor system simulation scenarios.

The RELAP-7 code utilizes the well-posed 7-equation two-phase flow model for compressible two-phase flow. Topological closure models used in the TRACE code have been reviewed and selected to reflect the progress made during the past decades and provide a basis for the closure correlations implemented in the RELAP-7 code. This document provides a summary on the closure correlations that are currently implemented in the RELAP-7 code. The closure correlations include sub-grid models that describe interactions between the fluids and the flow channel, and interactions between the two phases.

1 Introduction

The RELAP-7 (Reactor Excursion and Leak Analysis Program) code is the next generation nuclear reactor system safety analysis code being developed at Idaho National Laboratory (INL). The code is based on the INL's modern scientific software development framework MOOSE (Multi-Physics Object Oriented Simulation Environment) [1]. The overall design goal of RELAP-7 is to take advantage of the previous thirty years of advancements in computer architecture, software design, numerical integration methods, and physical models. The end result will be a reactor systems analysis capability that retains, and improves upon, RELAP5's [2] and TRACE's [3] abilities and extends the analysis capability for all reactor system simulation scenarios.

This document presents the topological closure correlations (those are dependent upon the two-phase flow topology) required to close the two-phase flow equation system. These include sub-grid models for interactions between the fluid and the flow channel (wall drag and wall heat transfer), and the interactions between the two phases (interfacial drag and heat/mass transfer). Some numerical treatments on code implementation will also be given.

2 Seven-Equation Two-Phase Flow Model

In this section, the one-dimensional seven-equation two-phase flow model is recalled first. In the seven-equation model, a set of balance equations for mass, momentum, and total energy are formulated for each of the two phases. An additional dynamic equation on volume fraction of the liquid phase is formulated to consider the evolution of volume fraction due to interactions between the two phases. To summarize, the one-dimensional seven-equation two-phase flow model is described in the following equations:

$$\begin{aligned}\frac{\partial \alpha_{liq} A}{\partial t} + u_{int} A \frac{\partial \alpha_{liq}}{\partial x} &= A\mu(p_{liq} - p_{vap}) \\ &\quad - \frac{\Gamma^{int}_{liq\to vap} A_{int} A}{\rho_{int}} - \frac{\Gamma^{wall}_{liq\to vap} P_{hf}}{\rho_{int}}\end{aligned} \tag{1}$$

$$\frac{\partial \left(\alpha\rho\right)_{liq} A}{\partial t} + \frac{\partial \left(\alpha\rho u\right)_{liq} A}{\partial x} = -\Gamma^{int}_{liq\to vap} A_{int} A - \Gamma^{wall}_{liq\to vap} P_{hf} \tag{2}$$

$$\begin{aligned}\frac{\partial \left(\alpha\rho u\right)_{liq} A}{\partial t} + \frac{\partial \alpha_{liq} A \left(\rho u^2 + p\right)_{liq}}{\partial x} &= p_{int} A \frac{\partial \alpha_{liq}}{\partial x} + p_{liq}\alpha_{liq}\frac{\partial A}{\partial x} \\ &\quad + A\lambda(u_{vap} - u_{liq}) \\ &\quad - \Gamma^{int}_{liq\to vap} A_{int} u_{int} A \\ &\quad - \Gamma^{wall}_{liq\to vap} u_{int} P_{hf} \\ &\quad - F_{\text{wall friction},liq} - F_{\text{friction},vap} \\ &\quad + \left(\alpha\rho\right)_{liq} A\boldsymbol{g}\cdot\hat{\boldsymbol{n}}_{axis}\end{aligned} \tag{3}$$

$$\begin{aligned}\frac{\partial \left(\alpha\rho E\right)_{liq} A}{\partial t} + \frac{\partial \alpha_{liq} u_{liq} A \left(\rho E + p\right)_{liq}}{\partial x} &= p_{int} u_{int} A \frac{\partial \alpha_{liq}}{\partial x} - \bar{p}_{int} A\mu(p_{liq} - p_{vap}) \\ &\quad + \bar{u}_{int} A\lambda(u_{vap} - u_{liq}) \\ &\quad + \Gamma^{int}_{liq\to vap} A_{int}\left(\frac{p_{int}}{\rho_{int}} - H_{liq,int}\right) A \\ &\quad - \Gamma^{wall}_{liq\to vap} H_{liq} P_{hf} \\ &\quad + Q_{int,liq} + Q^{conv}_{wall,liq} \qquad (4) \\ &\quad + \left(\alpha\rho u\right)_{liq} A\boldsymbol{g}\cdot\hat{\boldsymbol{n}}_{axis} \qquad (5)\end{aligned}$$

for the liquid phase, and

$$\frac{\partial \left(\alpha\rho\right)_{vap} A}{\partial t} + \frac{\partial \left(\alpha\rho u\right)_{vap} A}{\partial x} = \Gamma^{int}_{liq\rightarrow vap} A_{int} A + \Gamma^{wall}_{liq\rightarrow vap} P_{hf} \tag{6}$$

$$\begin{aligned}\frac{\partial \left(\alpha\rho u\right)_{vap} A}{\partial t} + \frac{\partial \alpha_{vap} A \left(\rho u^2 + p\right)_{vap}}{\partial x} &= p_{int} A \frac{\partial \alpha_{vap}}{\partial x} + p_{vap}\alpha_{vap}\frac{\partial A}{\partial x} \\ &+ A\lambda(u_{liq} - u_{vap}) \\ &+ \Gamma^{int}_{liq\rightarrow vap} A_{int} u_{int} A \\ &+ \Gamma^{wall}_{liq\rightarrow vap} u_{int} P_{hf} \\ &- F_{\text{wall friction},vap} - F_{\text{friction},liq} \\ &+ \left(\alpha\rho\right)_{vap} A\boldsymbol{g}\cdot\hat{\boldsymbol{n}}_{axis} \end{aligned} \tag{7}$$

$$\begin{aligned}\frac{\partial \left(\alpha\rho E\right)_{vap} A}{\partial t} + \frac{\partial \alpha_{vap} u_{vap} A \left(\rho E + p\right)_{vap}}{\partial x} &= p_{int} u_{int} A \frac{\partial \alpha_{vap}}{\partial x} - \bar{p}_{int} A \mu (p_{vap} - p_{liq}) \\ &+ \bar{u}_{int} A\lambda(u_{liq} - u_{vap}) \\ &- \Gamma^{int}_{liq\rightarrow vap} A_{int} \left(\frac{p_{int}}{\rho_{int}} - H_{vap,int}\right) A \\ &+ \Gamma^{wall}_{liq\rightarrow vap} H_{liq} P_{hf} \\ &+ Q_{int,vap} + Q_{wall,vap} + Q^{boil}_{wall,liq} \qquad (8) \\ &+ \left(\alpha\rho u\right)_{vap} A\boldsymbol{g}\cdot\hat{\boldsymbol{n}}_{axis} \qquad (9) \end{aligned}$$

for the vapor phase. More details on this set of equations can be found in the RELAP-7 theory manual [4]. To fully close this equation system, equations of state are needed to obtain the thermodynamic properties of steam (vapor) and water (liquid), as are constitutive transport properties. Additional *closure correlations* are required to model the interactions between the fluid to flow channel (e.g., wall friction and wall boiling), and the interactions between the two phases (e.g., interfacial friction and heat/mass transfer). These closure relations are sometimes called *topological* closure relations because they are strongly dependent upon the topology of the two-phase flow field; it is these closure correlations that are given in the remainder of this report. For RELAP-7 code development, the closure correlations from the TRACE system analysis code [3] will be used (to the extent that they conform to needs of the seven-equation two-phase model) for their wide coverage of thermal-hydraulics conditions of interest in reactor safety analysis. The following sections give detailed descriptions on the closure correlations implemented in the RELAP-7 code, including wall drag, interfacial drag, interfacial heat/mass transfer, and wall heat transfer. Unless explicitly stated otherwise, the original source for each closure correlation is the TRACE theory manual [3].

3 Wall Drag

In this section, the wall friction model will be discussed for both the single-phase and two-phase flow conditions. The single-phase flow condition will be discussed first, followed with the two-phase flow correlations, which rely on the single-phase wall friction model. The two-phase flow wall friction model will be discussed for both the pre-CHF and post-CHF flow conditions, and also for a special horizontal stratified flow condition. Transition between flow regimes will also be discussed.

3.1 Single-Phase Flow

For single-phase flow, the wall friction term is modeled as

$$F_{wall\,friction} = C_{wall}|u|uA\,, \tag{10}$$

where u is the velocity, and C_{wall} is the wall drag coefficient. Following the TRACE code [3], the wall drag coefficient is modeled as

$$C_{wall} = f_{wall}\frac{2\rho}{D_h}\,, \tag{11}$$

where f_{wall} is the Fanning friction factor[1], and D_h is the hydraulic diameter. As suggested in the TRACE code [3], the Churchill formula is used to calculate the wall friction factor for single-phase flow:

$$f_{wall} = 2\left[\left(\frac{8}{\mathrm{Re}}\right)^{12} + \frac{1}{(a+b)^{3/2}}\right]^{1/12}\,, \tag{12}$$

where

$$a = \left\{2.475\ln\left[\frac{1}{\left(\frac{7}{\mathrm{Re}}\right)^{0.9} + 0.27\left(\frac{\epsilon}{D_h}\right)}\right]\right\}^{16}\,, \tag{13}$$

and

$$b = \left(\frac{3.753\times10^4}{\mathrm{Re}}\right)^{16}\,, \tag{14}$$

with ϵ being the surface roughness.

The Reynolds number is computed as

$$\mathrm{Re} = \max\left(\frac{\rho|u|D_h}{\mu}, 10\right)\,, \tag{15}$$

where μ is the dynamic viscosity, and a lower limit of 10 is imposed.

[1]Note that the Fanning friction factor is equal to 1/4 times the Darcy-Weisbach friction factor.

3.2 Two-Phase Flow: Pre-CHF Flow Regimes

For two-phase flow regimes, the two-phase multiplier concept is used to determine the two-phase flow wall drag. By comparing the 7-equation model presented in the previous chapter and the traditional 6-equation two-fluid model used in the TRACE code, it can be observed that

$$F_{wall\ friction,liq} = AC_{wall,liq}u_{liq}|u_{liq}| \tag{16}$$

and

$$F_{wall\ friction,vap} = AC_{wall,vap}u_{vap}|u_{vap}|\,, \tag{17}$$

where $C_{wall,liq}$ and $C_{wall,vap}$ are the phasic wall drag coefficients used in the TRACE code, A is the pipe cross-sectional area, and u_{liq} and u_{vap} are the phasic velocities. For pre-CHF two-phase flow regimes, wall drag coefficients are modeled in bubbly/slug and annular/mist flow regimes. For all pre-CHF two-phase flow regimes, it is assumed that all of the wall drag is applied to the liquid phase alone.

3.2.1 Bubbly/Slug Flow Regime

When wall nucleate boiling effect is not considered, the liquid phase wall drag coefficient is modeled as

$$C_{wall,liq} = f_{wall,liq}\frac{2\rho_{liq}}{D_h}\,, \tag{18}$$

with $f_{wall,liq}$ calculated from the Churchill formula using the liquid phase Reynolds number:

$$\mathrm{Re}_{2\Phi,liq} = \frac{(1-\alpha_{vap})\rho_{liq}|u_{liq}|D_h}{\mu_{liq}}\,. \tag{19}$$

to consider the two-phase flow vapor volume fraction effect. When nucleate boiling effect is considered, following the TRACE code [3], a correction factor is introduced, and the wall drag coefficient is then modeled as

$$C_{wall,liq} = f_{wall,liq}\frac{2\rho_{liq}}{D_h}(1+C_{NB})^2\,, \tag{20}$$

where the empirical coefficient C_{NB} is given as

$$C_{NB} = \min\left\{2,\ 155\frac{d_B}{D_h}[\alpha_{vap}(1-\alpha_{vap})]^{0.62}\right\}\,, \tag{21}$$

where

$$\frac{d_B}{D_h} = 0.015\left(\frac{\sigma}{\tau_w D_h}\right)^{0.5}\,, \tag{22}$$

and

$$\tau_w = \frac{f_{wall,liq}}{2}\rho_{liq}u_{liq}^2\,. \tag{23}$$

The gas phase wall drag is assumed to be zero: $C_{wall,vap} = 0$.

3.2.2 Annular/Mist Flow Regime

Similar to the TRACE code [3], in the annular/mist flow regime, if the channel surface is considered to be fully covered by liquid film, the wall drag coefficient for the liquid phase is modeled as

$$C_{wall,liq} = f_{film}\frac{2\rho_{liq}}{D_h}\,, \tag{24}$$

where f_{film} is the friction factor for the annular flow regime and is given by a power law combination of the laminar and turbulent values:

$$f_{film} = (f_{lam}^3 + f_{turb}^3)^{1/3}\,. \tag{25}$$

Here the friction factor for the laminar regime is modeled as

$$f_{lam} = \begin{cases} \frac{16}{\mathrm{Re}_{2\Phi,liq}} & \alpha_{vap} \le 0.95 \\ \frac{\left[16+8\left(\frac{\alpha_{vap}-0.95}{0.99-0.95}\right)\right]}{\mathrm{Re}_{2\Phi,liq}} & 0.95 < \alpha_{vap} < 0.99 \\ \frac{24}{\mathrm{Re}_{2\Phi,liq}} & \alpha_{vap} \ge 0.99 \end{cases}\,. \tag{26}$$

The linear interpolation between vapor volume fraction 0.95 and 0.99 reflects the transition between pipe geometry correlation and parallel plate geometry, which is more appropriate for thinner film with void fraction larger than 0.99. The friction factor for the turbulent regime is modeled as

$$f_{turb} = \frac{1}{\left\{3.6\log_{10}\left[\frac{6.9}{\mathrm{Re}_{2\Phi,liq}} + \left(\frac{\epsilon/D}{3.7}\right)^{1.11}\right]\right\}^2}\,. \tag{27}$$

In these correlations, $\mathrm{Re}_{2\Phi,liq}$ is calculated using equation (19). The vapor phase wall drag is assumed to be zero, i.e., $C_{wall,vap} = 0$, if the channel surface is fully covered by liquid film.

When the channel surface is considered to be partially covered by liquid film, taken as the condition wherein liquid film is present with thickness smaller than 25 μm, the wall drag coefficient for the liquid phase is modeled as

$$C_{wall,liq} = f_{wet}f_{film}\frac{2\rho_{liq}}{D_h}\,, \tag{28}$$

where

$$f_{wet} = \frac{(1-\alpha_{vap})D_h}{4(25\times10^{-6})}\,. \tag{29}$$

In this case, the vapor phase wall drag coefficient is no longer zero and is modeled as

$$C_{wall,vap} = (1-f_{wet})f_{2\Phi,vap}\frac{2\rho_{vap}}{D_h}\,, \tag{30}$$

with $f_{2\Phi,vap}$ denoting the vapor phase friction factor, which is computed with the Churchill formula with the vapor phase Reynolds number

$$\mathrm{Re}_{2\Phi,vap} = \frac{\alpha_{vap}\rho_{vap}|u_{vap}|D_h}{\mu_{vap}}\,. \tag{31}$$

3.2.3 Transition between Bubbly/Slug and Annular/Mist Flow Regimes

Following the TRACE code [3], a smooth transition from the bubbly/slug flow regime to the annular/mist flow regime is used. The transition is assumed to occur between vapor volume fractions of 0.8 and 0.9; here, the liquid phase wall drag coefficient is modeled as

$$C_{wall,liq} = wf_{BS}C_{wall,liq,BS} + (1-wf_{BS})C_{wall,liq,AM}\,, \tag{32}$$

where the weight factor is defined as

$$wf_{BS} = \frac{0.9-\alpha_{vap}}{0.9-0.8}\,. \tag{33}$$

3.2.4 Horizontal Stratified Flow

For horizontal stratified flow condition, both phases are in contact with the channel wall, so the wall drag coefficient is modeled separately for each phase. At first, for phase k = {*liq, vap*}, the the wall frictional factor is calculated from the Churchill formula with the phasic Reynolds number, Re_k, which is defined as

$$\mathrm{Re}_k = \frac{\rho_k u_k D_{h,k}}{\mu_k}\,, \tag{34}$$

with $D_{h,k}$ being the phasic hydraulic diameter. Following the definition used in TRACE [3], the two phasic hydraulic diameters are defined as

$$D_{h,liq} = \frac{4A_{liq}}{S_{liq}} = \frac{4A\alpha_{liq}}{S_{liq}} \tag{35}$$

and

$$D_{h,vap} = \frac{4A_{vap}}{S_{vap} + S_{int}} = \frac{4A\alpha_{vap}}{S_{vap} + S_{int}} \,. \tag{36}$$

As shown in Figure 1, S_{liq}, S_{vap}, and S_{int} can be obtained as

$$S_{liq} = D\theta \,, \tag{37}$$

$$S_{vap} = D(\pi - \theta) \,, \tag{38}$$

and

$$S_{int} = D \sin\theta \,, \tag{39}$$

where θ is in radians and is computed as

$$\theta = \cos^{-1}\left(\frac{D/2 - h}{D/2}\right) = \cos^{-1}\left(1 - \frac{2h}{D}\right) \,. \tag{40}$$

The depth of the liquid phase, h, can be obtained as a curve-fitting function for round pipe as

$$\frac{h}{D} = \begin{cases} 1 - 7.0612668\alpha_{vap} & \alpha_{vap} \leq 0.001 \\ 1.0 - a_1\alpha_{vap}^{2/3} - a_2\alpha_{vap} - a_3\alpha_{vap}^2 & 0.001 < \alpha_{vap} \leq 0.5 \\ b_1\alpha_{liq}^{2/3} + b_2\alpha_{liq} + b_3\alpha_{liq}^2 & 0.5 < \alpha_{vap} \leq 0.999 \\ 7.0612668\alpha_{liq} & \alpha_{vap} > 0.999 \end{cases} \,, \tag{41}$$

where $a_1 = 0.70269591$, $a_2 = 0.034146667$, $a_3 = 0.161023911$, $b_1 = 0.70269591$, $b_2 = 0.034146667$, and $b_3 = 0.161023911$.

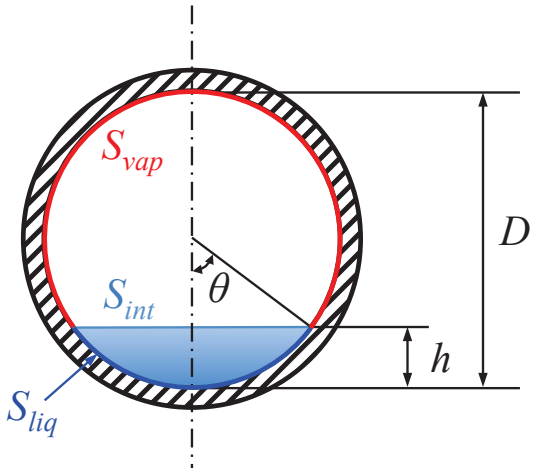

Figure 1. Schematic drawing of the horizontal stratified flow.

Then, considering the wetted perimeter for each phase, the wall drag coefficients are modeled as

$$C_{wall,k} = f_{wall,k}\frac{2\rho_k}{D_{h,wet}} = f_{wall,k}\frac{\rho_k}{2}\frac{S_k}{A}\,, \tag{42}$$

where

$$D_{h,wet} = \frac{4A}{S_k}\,. \tag{43}$$

That is,

$$C_{wall,liq} = f_{wall,liq}\frac{\rho_{liq}}{2}\frac{S_{liq}}{A} = f_{wall,liq}\frac{2\rho_{liq}}{D}\frac{\theta}{\pi}\,, \tag{44}$$

and

$$C_{wall,vap} = f_{wall,vap}\frac{\rho_{vap}}{2}\frac{S_{vap}}{A} = f_{wall,vap}\frac{2\rho_{vap}}{D}\frac{(\pi-\theta)}{\pi}\,. \tag{45}$$

It must be noted that all previous derivations are based on a round pipe assumption.

3.2.5 Transition between Horizontal Stratified and Non-Stratified Flow

If the flow regime is considered to be in transition between stratified and non-stratified condition, a linear interpolation is used:

$$C_{wall,k} = wf_{strat}C_{wall,k,strat} + (1 - wf_{strat})C_{wall,k,non-strat}\,, \tag{46}$$

where $C_{wall,k,strat}$ and $C_{wall,k,non-strat}$ are wall drag coefficients for stratified and non-stratified conditions, respectively. Following the TRACE manual [3], the weighting factor, wf_{strat}, is determined from several factors:

$$wf_{strat} = wf_{TD}wf_{CW}wf_{CCFL}\,, \tag{47}$$

where wf_{TD} is the weighting factor for the Taitel-Dukler transition from stratified flow condition, wf_{CF} is the weighting factor for mass flux, and wf_{CCFL} is the weighting factor for counter-current flow limit.

The weighting factor for the Taitel-Dukler transition from stratified flow condition, wf_{TD}, is defined as

$$wf_{TD} = \max\left[0, \min\left(1,\, 2 - \frac{|u_r|}{u_{r,crit}}\right)\right]\,, \tag{48}$$

with $u_r = u_{vap} - u_{liq}$, and

$$u_{r,crit} = \left(1 - \frac{h_l}{D}\right)\left[\frac{g\Delta\rho\cos\phi A_{vap}}{\rho_g(dA_l/dh_l)}\right]^{1/2}\,, \tag{49}$$

where ϕ is the pipe inclination angle (for example, $\phi = 0$ for horizontal pipe and $\pi/2$ for vertical pipe), and (dA_l/dh_l) is the derivative of liquid flow area with respect to height, which is obtained as

$$\frac{dA_l}{dh_l} = \max\left\{ D\left[1 - \left(\frac{2h_l}{D} - 1\right)^2\right]^{1/2}, 0.0001D \right\} . \tag{50}$$

As in the TRACE manual [3], the weighting factor for mass flux, wf_{CW}, is calculated as

$$wf_{CW} = \max\left[0, \min\left(1, \frac{2700 - G}{2700 - 2000}\right)\right] , \tag{51}$$

where G is the total mass flux of the two-phase mixture.

Again as in the TRACE manual [3], the weighting factor for counter-current flow limit, wf_{CCFL}, is calculated as

$$wf_{CCFL} = \max\left[0, \min\left(1, \frac{1.2 - \left(j^*_{vap}\right)^{1/2} - \left(j^*_{liq}\right)^{1/2}}{1.2 - 0.65}\right)\right] , \tag{52}$$

with the non-dimensional superficial phasic velocities defined as

$$j^*_k = |j_k| \left(\frac{\rho_k}{g\Delta\rho D}\right)^{1/2} . \tag{53}$$

Here the superficial phasic velocity is defined by $j_k = \alpha_k u_k$.

This concludes the wall drag model for two-phase flow for pre-CHF flow regimes, including bubbly/slug, annular/mist, transition between bubbly/slug and annular/mist, horizontal stratified flow, and transition between horizontal stratified and non-stratified flow conditions.

3.3 Two-Phase Flow: Post-CHF Flow Regimes

For post-CHF conditions, wall drag is modeled for two flow regimes, i.e., the inverted annular and dispersed flow regimes. A linear interpolation is used in the transitional region between these two regimes.

3.3.1 Inverted Annular Flow

The inverted annular flow regime is applied for vapor volume fraction less than 0.6 under the post-CHF conditions. In this regime, it is assumed that only the vapor phase is in

contact with the wall, and the wall-to-liquid drag is zero, which leads to $C_{wl} = 0$. For the wall drag to the vapor phase, a similar two-phase multiplier concept is used. The wall drag coefficient for the vapor phase is modeled as

$$C_{wall,vap} = \Phi_{vap}^2 \left[\frac{2 f_{2\Phi,vap} \alpha_{vap}^2 \rho_{vap}}{D_h} \right] . \tag{54}$$

By analogy with annular flow, the two-phase multiplier for the inverted annular flow is

$$\Phi_{vap}^2 = \frac{1}{\alpha_{vap}^2} , \tag{55}$$

so the wall coefficient is

$$C_{wall,vap} = f_{2\Phi,vap} \frac{2\rho_{vap}}{D_h} . \tag{56}$$

Here, the friction factor $f_{2\Phi,vap}$ is the Fanning friction factor calculated from the Churchill formula, Equation (12), with

$$\mathrm{Re}_{2\Phi,vap} = \frac{|G_{vap}| D_h}{\mu_{vap}} = \frac{\alpha_{vap} \rho_{vap} |u_{vap}| D_h}{\mu_{vap}} . \tag{57}$$

3.3.2 Dispersed Flow

The dispersed flow regime is applied for vapor volume fraction larger than 0.9 under the post-CHF conditions. The wall drag coefficient for the dispersed flow regime is modeled as

$$C_{wall,vap} = f_{pg} \frac{2\rho_{vap}}{D_h} , \tag{58}$$

where f_{pg} is the effective friction fraction for dilute suspensions:

$$f_{pg} = f_{wall,vap} \left[1 + \min(12, \mathrm{LF}) \right]^{0.3} . \tag{59}$$

In this equation, LF is the loading factor that is calculated as

$$\mathrm{LF} = \frac{(1 - \alpha_{vap}) \rho_{liq} u_{liq}}{\alpha_{vap} \rho_{vap} u_{vap}} . \tag{60}$$

The vapor phase wall friction factor, $f_{wall,vap}$, is calculated from the Churchill formula, Equation (12), similar to the inverted annular flow condition.

3.3.3 Transition between Inverted Annular and Dispersed Flow

Under post-CHF flow conditions, when the vapor volume fraction is between 0.6 and 0.9, a linear interpolation method is used. A dispersed flow weighting factor is first defined as

$$wf_{DF} = \frac{\alpha_{vap} - 0.6}{0.9 - 0.6}\,, \tag{61}$$

and then the wall drag coefficient for this transitional region is interpolated as

$$C_{wall,vap} = (1 - wf_{DF})\, C_{wall,vap,IA} + wf_{DF} C_{wall,vap,DF}\,, \tag{62}$$

where the subscripts IA and DF represent inverted annular flow and dispersed flow conditions, respectively.

4 Interfacial Drag

By comparing the 7-equation model presented in Section 2 and the 6-equation two-fluid model used in the TRACE code [3], it can be found that

$$F_{friction,vap} = -F_{friction,liq} = AC_i u_r |u_r| \,, \tag{63}$$

where A is the pipe cross-sectional area, C_i is the interfacial drag coefficient, and u_r is the relative velocity between the two phases:

$$u_r = u_{vap} - u_{liq} \,. \tag{64}$$

All correlations discussed in this section closely follow those used in the TRACE code [3].

4.1 Pre-CHF Flow Regimes

For pre-CHF regimes in vertical pipes/bundles, interfacial drag is modeled in three major regimes: bubbly, cap/slug, and annular/mist. The bubbly and slug flow regimes are grouped together using a similar approach that is based on the drift-flux model concept.

4.1.1 Bubbly/Slug Flow

For the combined bubbly/slug flow regime, the interfacial drag coefficient, C_i, is modeled as

$$C_{i,BS} = \frac{\alpha_{vap}(1-\alpha_{vap})^3 g \Delta\rho}{\bar{v}_{gj}^2} P_s \,, \tag{65}$$

where the subscript BS stands for the combined bubbly and slug flow regimes, P_S is the profile slip factor, $\bar{v}_{gj}$ is the weighted area-average value of the drift velocity, and $\Delta\rho$ is the density difference between the two phases: $\Delta\rho = \rho_{liq} - \rho_{vap}$.

The profile slip factor is calculated as

$$P_s = \frac{\left(\frac{1-C_0\alpha_{vap}}{1-\alpha_{vap}} u_{vap} - C_0 u_{liq}\right)^2}{u_r^2} \,. \tag{66}$$

In code implementation, a small value, 10^{-8}, is added into the denominator. The distribution coefficient, C_0, and the weighted area-average value of the drift velocity, $\bar{v}_{gj}$, are both dependent on flow regime and will be discussed for each.

4.1.1.1 Pipe Geometry

If a pipe flow condition is concerned, the two drift flux model related parameters $\bar{v}_{gj}$ and C_0 are modeled separately in both the dispersed bubbly flow and cap/slug flow conditions. If the flow channel is of rod bundle type, models for these two parameters are discussed later in this section.

For the dispersed bubbly flow regime in a pipe, these two parameters are modeled as

$$(\bar{v}_{gj})_{DB} = \sqrt{2}\left(\frac{\sigma g \Delta\rho}{\rho_{liq}^2}\right)^{1/4} \tag{67}$$

and

$$C_{0,DB} = 1.2 - 0.2\sqrt{\frac{\rho_{vap}}{\rho_{liq}}}\,, \tag{68}$$

where σ is the surface tension of the interface, and subscript DB represents the dispersed bubbly flow regime.

For the cap/slug flow regime, the distribution coefficient, C_0, is modeled the same as in the dispersed bubbly flow regime: $C_{0,CS} = C_{0,DB}$. The subscript CS represents the cap/slug flow regime. For the cap/slug flow regime, the weighted drift velocity is given by

$$(\bar{v}_{gj})_{CS} = \bar{v}_{gj}^{+}\left(\frac{\sigma g \Delta\rho}{\rho_{liq}^2}\right)^{1/4}\,, \tag{69}$$

where the non-dimensional drift velocity is modeled as

$$\bar{v}_{gj}^{+} = 0.0019\left(\min[30, D_h^*]\right)^{0.809}\left(\frac{\rho_{vap}}{\rho_{liq}}\right)^{-0.157} N_{\mu,liq}^{-0.562}\,. \tag{70}$$

Here, the non-dimensional hydraulic diameter is given as

$$D_h^* = \frac{D_h}{\sqrt{\frac{\sigma}{g\Delta\rho}}}\,, \tag{71}$$

and the liquid viscosity number is defined as

$$N_{\mu,liq} \equiv \frac{\mu_{liq}}{\left(\rho_{liq}\sigma\sqrt{\frac{\sigma}{g\Delta\rho}}\right)^{1/2}}\,. \tag{72}$$

The quantity $\sqrt{\frac{\sigma}{g\delta\rho}}$ is a *capillary number*, Ca, which will recur subsequently, so for convenience, this definition shall be made:

$$\mathrm{Ca} = \sqrt{\frac{\sigma}{g\Delta\rho}}\,.$$

A transition region is added between the dispersed bubbly and cap/slug flow regimes. In this transition region, a simple linear interpolation is used to model the weighted drift velocity:

$$\bar{v}_{gj} = wf_{DB}\left(\bar{v}_{gj}\right)_{DB} + \left(1 - wf_{DB}\right)\left(\bar{v}_{gj}\right)_{CS} . \tag{73}$$

The weighted drift velocity $\left(\bar{v}_{gj}\right)_{DB}$ and $\left(\bar{v}_{gj}\right)_{CS}$ are calculated from Equations (67) and (69), respectively. The linear interpolation coefficient wf_{DB} is calculated as

$$wf_{DB} = \frac{\alpha_{vap,CS} - \alpha_{vap}}{\alpha_{vap,CS} - \alpha_{vap,DB}} , \tag{74}$$

where

$$\alpha_{vap,DB} = 0.2 \ \min\left[1, \frac{T_{sat} - T_l}{5}\right] , \tag{75}$$

and

$$\alpha_{vap,CS} = \alpha_{vap,DB} + 0.1 , \tag{76}$$

with $T_{sat} = T_{int}$.

4.1.1.2 Rod Bundle Geometry

For rod bundle geometry, the Bestion model is recommended in the TRACE code [3] to calculate $\bar{v}_{gj}$, which is

$$\bar{v}_{gj} = 0.188\sqrt{g\Delta\rho D_h/\rho_{vap}} . \tag{77}$$

The distribution parameter, C_0, for rod bundle geometry is simply set to be 1.

4.1.2 Annular/Mist Flow

For the annular/mist flow regime, the interfacial drag comes from two parts: the interfacial drag between the liquid film and the vapor core, and the interfacial drag between the liquid droplets and the vapor core.

Considering the velocity difference between the liquid film and the liquid droplets entrained in the vapor core, and following the TRACE code [3], the overall interfacial drag coefficient for the annular/mist flow regime is modeled as

$$C_{i,AM} = C_{i,film} + C_{i,drop}\frac{u_{r,d}^2}{\left(u_{vap} - u_{liq}\right)^2} , \tag{78}$$

where $C_{i,film}$ and $C_{i,drop}$ are the interfacial drag coefficients for the liquid film and droplets, respectively, and $u_{r,d}$ is the droplet relative velocity. In code implementation, the magnitude of $u_{vap} - u_{liq}$ is defined to be larger than 10^{-6} m/s. The interfacial drag coefficient for the liquid film part is modeled as

$$C_{i,film} = f_{i,film} A'''_{i,film} \frac{1}{2} \rho_{vap} \,. \tag{79}$$

Here, the specific interfacial area (interfacial area per unit volume) is computed from

$$A'''_{i,film} = \frac{4}{D_h} \sqrt{\alpha_{vap}} \,, \tag{80}$$

and the friction factor for the liquid film is approximated by

$$f_{i,film} = 0.005[1 + 75(1 - \alpha_{vap})] \,. \tag{81}$$

For the interfacial drag between the liquid droplets and the vapor core, the fraction of the liquid flow that is entrained as droplets in the vapor core must be estimated first. For small diameter pipes ($D_h \leq 3.2\,\mathrm{cm}$), the entrainment fraction is modeled as

$$E_\infty = \tanh\left[7.25 \times 10^{-7}\, \mathrm{We}_{vap}^{1.25}\ \min(6400, \mathrm{Re}_f)^{0.25}\right] \,, \tag{82}$$

where the liquid film Reynolds number is defined as

$$\mathrm{Re}_f = \frac{(1 - \alpha_{vap}) \rho_{liq} u_{liq} D_h}{\mu_{liq}} \,, \tag{83}$$

and the effective Weber number for entrainment is defined as

$$\mathrm{We}_{vap} = \frac{\rho_{vap} j_{vap}^2 D_h}{\sigma} \left(\frac{\Delta\rho}{\rho_{vap}}\right)^{1/3} \,, \tag{84}$$

with j_{vap} being the superficial velocity of the vapor phase. The superficial phasic velocities, or phasic volumetric fluxes, are defined to be

$$j_k = \alpha_k u_k$$

for $k = \{liq, vap\}$.

For large diameter pipes, ($D_h > 3.2\,\mathrm{cm}$), the entrained fraction is modeled as

$$E_\infty = 0.015 + 0.44 \log_{10}\left[0.9245 \left(\frac{\pi_2}{\pi_{2,crit}}\right)^2\right] \,, \tag{85}$$

where π_2 is the non-dimensional vapor velocity that is defined as

$$\pi_2 = \frac{j_{vap} \mu_{vap}}{\sigma} \sqrt{\frac{\rho_{vap}}{\rho_{liq}}} \,, \tag{86}$$

and $\pi_{2,crit} = 2.46 \times 10^{-4}$ is the inception criteria for liquid droplet entrainment. In code implementation, the value of $0.9245\,(\pi_2/\pi_{2,crit})^2$ is limited to be larger than 10^{-10}, and the final value of entrained fraction, E_∞, is limited to be larger or equal to zero.

Following the TRACE code [3], the interfacial drag coefficient for the droplets is modeled as

$$C_{i,drop} = C_D A_d''' \frac{1}{2} \rho_{vap} \tag{87}$$

$$= C_D \ \rho_{vap} \frac{3\alpha_c \alpha_d}{4 d_d} \,, \tag{88}$$

where α_c is the volume fraction of the annular core region (containing vapor and droplets), and α_d is the fraction of the annular core occupied by the droplets alone. For this equation, the following relation for the projected area of droplets per unit mixture volume was used:

$$A_d''' = \frac{3}{2} \frac{\alpha_{vap}\alpha_d}{(1-\alpha_d) d_d} \,. \tag{89}$$

The drop drag coefficient is modeled as

$$C_D = \frac{24}{\mathrm{Re}_d} \left(1 + 0.1 \mathrm{Re}_d^{0.75}\right) \,, \tag{90}$$

with the drop Reynolds number defined as

$$\mathrm{Re}_d = \frac{\rho_{vap} |u_{vap} - u_d| d_d}{\mu_m} \,. \tag{91}$$

Here, d_d is the droplet Sauter mean diameter (discussed later), and the mixture viscosity is given by

$$\mu_m = \frac{\mu_{vap}}{(1-\alpha_d)^{2.5}} \,. \tag{92}$$

The fraction of the annular vapor core occupied by the droplets is approximated by

$$\alpha_d = E_\infty \frac{|j_{liq}|}{|j_{vap}|} \,. \tag{93}$$

To avoid numerical issues, in code implementation, the denominator is modified to $|j_{vap}| + 10^{-6}$. The value of α_d is also limited by

$$\alpha_d \leq E_\infty (1 - \alpha_{vap}) \,, \tag{94}$$

where again, j_{liq} and j_{vap} are the superficial velocities of the two phases. The Sauter mean diameter is modeled as

$$d_d = 0.008 \left(\frac{\sigma}{\rho_{vap} j_{vap}^2}\right) \mathrm{Re}_{vap}^{2/3} \left(\frac{\mu_{vap}}{\mu_{liq}}\right)^{2/3} \left(\frac{\rho_{vap}}{\rho_{liq}}\right)^{-1/3} \,, \tag{95}$$

where the gas Reynolds number is defined as

$$\mathrm{Re}_{vap} = \frac{\rho_{vap}|j_{vap}|D_h}{\mu_{vap}}\,. \tag{96}$$

In addition, the Sauter mean diameter is limited to be

$$84\mu\mathrm{m} \le d_d \le 4\,\mathrm{mm}\,. \tag{97}$$

The drop relative velocity, $u_{r,d} \equiv u_{vap} - u_d$, is modeled as

$$u_{r,d} = \begin{cases} 1.718\sqrt{d_d}\left[\frac{g\Delta\rho}{\rho_{vap}}\right]^{1/2}(1-\alpha_d)^{1.5} & d_d \le d_{d,Newton} \\ \sqrt{2}\left[\frac{\sigma g\Delta\rho}{\rho_{vap}^2}\right]^{1/4}(1-\alpha_d)^{1.5} & d_d > d_{d,Newton} \end{cases}, \tag{98}$$

with

$$d_{d,Newton} = 0.678\sqrt{\frac{\sigma}{g\Delta\rho}} = 0.678\mathrm{Ca}\,. \tag{99}$$

When $u_{r,d}$ is used to calculate droplet Reynolds number, its value is also defined to be larger than $10^{-6}\,\mathrm{m/s}$ to avoid a zero-valued Reynolds number that causes numerical issues when evaluating the drop drag coefficient, C_D.

4.1.3 Mixing of Bubbly/Slug and Annular/Mist Flows

Finally, in order to avoid a discontinuous change of the interfacial drag coefficient between the combined bubbly/slug flow regime and the annular/mist flow regime, the interfacial coefficient is averaged using a simple power law weighting scheme:

$$C_i = \sqrt{C_{i,BS}^2 + C_{i,AM}^2}\,, \tag{100}$$

where the subscripts BS and AM stand for bubbly/slug and annular/mist flow conditions, respectively.

4.1.4 Horizontal Stratified Flow

For horizontal stratified flow conditions, similar to the TRACE code [3], the interfacial drag coefficient is given as

$$C_{i,strat} = \frac{1}{2}\rho_{vap} f_i A_i'''\,. \tag{101}$$

The interfacial area per unit volume is defined as

$$A_i''' = \frac{S_{int}}{A}\,, \tag{102}$$

with S_{int} defined the same as in Equation (39). Following the TRACE code [3], the interfacial friction factor is given as

$$f_i = 1.84 f_{wall,vap} \,, \tag{103}$$

where $f_{wall,vap}$ is the single-phase wall drag friction factor for the gas phase. Its value is evaluated using the Churchill formula with the gas phase Reynolds number,

$$\mathrm{Re}_{vap} = \frac{\rho_{vap} u_{vap} D_{h,vap}}{\mu_{vap}} \,, \tag{104}$$

where the gas phase hydraulic diameter $D_{h,vap}$ is calculated using Equation (36).

4.1.5 Transition between Horizontal Stratified and Non-Stratified Flow

If the flow regime is considered to be in a transition between stratified and non-stratified condition, a power law based interpolation is used:

$$C_i = C_{i,strat}^{n} C_{i,non-strat}^{1-n} \,, \tag{105}$$

where subscripts $strat$ and $non - strat$ stand for stratified flow and non-stratified flow conditions, respectively. The exponent, n, is set to wf_{strat}, definded in Equation (47).

This concludes the interfacial drag model in flow channels for pre-CHF flow conditions, including bubbly/slug, annular/mist, horizontal stratified flow, and transitions between these flow regimes.

4.2 Post-CHF Flow Regimes

The post-CHF regimes are defined when the surface temperature exceeds the Leidenfrost point, where the liquid phase cannot contact the hot surface. Similar to the TRACE code [3], the post-CHF regimes take place between the bottom quench front and the top quench front. The post-CHF flow regimes include inverted annular, inverted slug, and dispersed flow regimes. Similar to the TRACE code [3], the post-CHF flow regimes are simply void-fraction-dependent, Figure 2.

4.2.1 Inverted Annular Flow

For the inverted annular regime that is defined with void fraction below 0.6, the interfacial drag coefficient is given by

$$C_{i,IA} = \frac{1}{2} \rho_{vap} f_{i,IA} A_i''' \,, \tag{106}$$

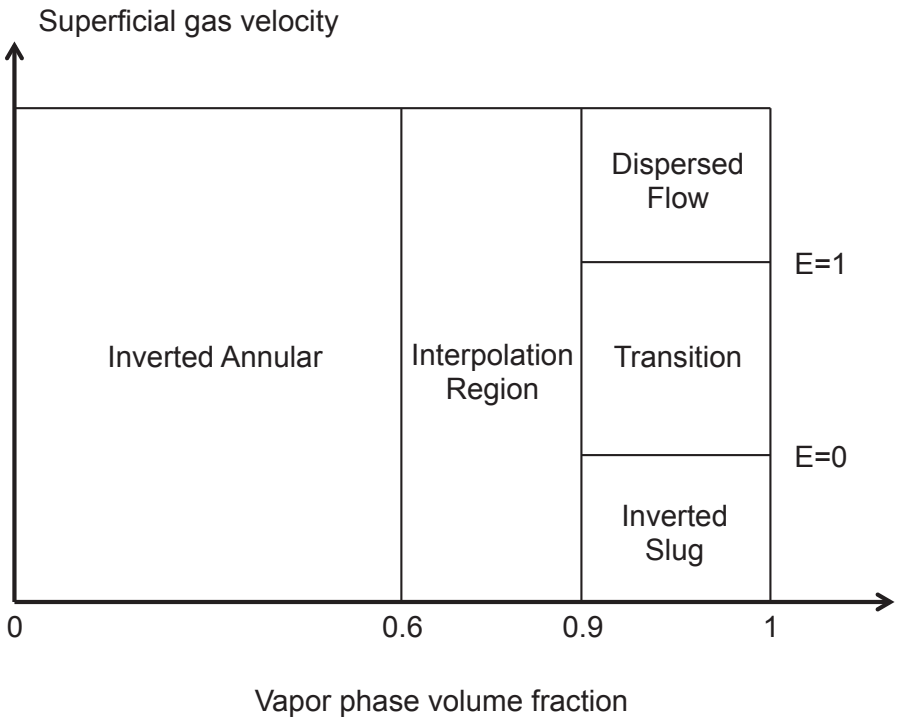

Figure 2. Post-CHF flow regime map [3].

where the subscript IA represents inverted annular flow condition. A_i''' is the interfacial area per unit volume and $f_{i,IA}$ is the interfacial friction factor. Assuming the liquid core is circular, the interfacial area per unit volume can be calculated as

$$A_i''' = 4\frac{\sqrt{1-\alpha_{vap}}}{D_h}\,. \tag{107}$$

The interfacial friction factor, $f_{i,IA}$, is calculated as a power-law-averaged value of both the smooth and wavy interface conditions:

$$f_{i,IA} = \sqrt{f_{i,smooth}^2 + f_{i,wavy}^2}\,, \tag{108}$$

where $f_{i,smooth}$ is for the laminar flow with a smooth interface, and $f_{i,wavy}$ is for the case with a way interface:

$$f_{i,smooth} = \frac{144}{(\delta^*)^3}\,, \tag{109}$$

$$f_{i,wavy} = 0.35\left(\frac{\delta}{\mathrm{La}}\right)^{0.72}\,. \tag{110}$$

The vapor film thickness is calculated as

$$\delta = \frac{D_h}{2}\left(1 - \sqrt{1-\alpha_{vap}}\right) \tag{111}$$

for tube geometry, and

$$\delta = \frac{D_h}{2}\left\{\sqrt{1+\alpha_{vap}\left[\frac{4}{\pi}\left(\frac{P}{D_r}\right)^2 - 1\right]} - 1\right\} \tag{112}$$

for rod bundle geometry. The non-dimensional vapor film thickness for evaluating the smooth interface interfacial friction factor is

$$\delta^* = \delta\left(\frac{\rho_{vap} g \Delta\rho}{\mu_{vap}^2}\right)^{1/3}. \tag{113}$$

The Laplace number is given by

$$\mathrm{La} = \sqrt{\frac{\sigma}{g\Delta\rho}}. \tag{114}$$

4.2.2 Inverted Slug Flow

For the inverted slug regime, the interfacial drag coefficient is given by

$$C_{i,IS} = \frac{1}{24}\frac{\rho_{vap}}{La}\frac{1-\alpha_{vap}}{\alpha_{vap}^{1.8}}, \tag{115}$$

following the recommendation made in the TRACE manual [3] that the coeffcient has been adjusted to better match FLECHT-SEASET high flooding rate reflood data.

4.2.3 Dispersed Flow

For the post-CHF dispersed flow regime, the interfacial drag coefficient is given by

$$C_{i,DF} = \frac{1}{2}\rho_{vap} C_{D,MP} A_p''', \tag{116}$$

where $C_{D,MP}$ is the drag coefficient corrected from multi-particle effects and A_p''' is the projected area per unit volume. The projected area per unit volume is calculated from the droplet Sauter mean diameter by

$$A_p''' = \frac{6(1-\alpha_{vap})}{4 d_{SM}}. \tag{117}$$

The Sauter mean diameter is estimated as about one-third of the maximum droplet diameter:

$$d_{SM} = \frac{1}{3} d_{max} \,. \tag{118}$$

The maximum droplet diamter is modeled differently for downflow and upflow conditions. For downflow condition, the maximum droplet diameter is estimated as

$$d_{max,down} = \min \left[3.52\mathrm{La}, D_h \right] \,. \tag{119}$$

For upflow condition, the maximum droplet diameter is estimated as

$$d_{max,up} = \min \left[5.07\mathrm{La} N_{\mu g}^{0.176}, \frac{18\sigma}{\rho_{vap} j_{vap}^2}, d_{max,down} \right] \,. \tag{120}$$

The multi-particle drag coefficient can be obtained from the single-particle model:

$$C_{D,MP} = \frac{C_{D,SP}}{\alpha_{vap}^{1.8}} \,. \tag{121}$$

The single-partical drag coefficient is calculated as

$$C_{D,SP} = \max \left[\frac{24}{\mathrm{Re}_d} \left(1 + 0.15 \mathrm{Re}_d^{0.687} \right), 0.44 \right] \,, \tag{122}$$

where the drop Reynolds number is defined by

$$Re_d = \frac{\rho_{vap} V_r d_{SM}}{\mu_{vap,film}} \,. \tag{123}$$

The relative velocity, V_r, is calculated as

$$V_r = \max \left[\frac{|u_{vap} - u_{liq}|}{\alpha_{vap}^{1.4}}, V_\infty \right] \,, \tag{124}$$

where V_∞ is the terminal velocity for large spherical drops. The vapor-phase viscosity, $\mu_{vap,film}$, should be estimated at the film temperature given by

$$T_{film} = \frac{T_{vap} + T_{sat}}{2} \,. \tag{125}$$

The non-dimensional terminal velocity for large spherical drops is modeled as

$$V_\infty^* = 0.693 \left(r^* \right)^{0.858} \,, \tag{126}$$

with

$$V_\infty^* = V_\infty \left[\frac{\rho_{vap}^2}{\mu_{vap} g \Delta\rho} \right]^{1/3} \,, \tag{127}$$

and

$$r^* = r \left[\frac{\rho_{vap} g \Delta\rho}{\mu_{vap}^2} \right]^{1/3} \,, \tag{128}$$

where r is the droplet radius.

4.2.4 Transition between Inverted Annular and Inverted Slug Flow Regimes

For void fractions between 0.6 and 0.9 under post-CHF condition, an interpolation region is applied between the inverted annular and inverted slug flow regimes. In this transition regime, the interfacial drag coefficient is computed as

$$C_i = wf_{IA} C_{i,IA} + (1 - wf_{IA}) C_{i,IS} \,, \tag{129}$$

where wf_{IA} is a spline weighting factor for inverted annular flow, given by

$$wf_{IA} = x(2 - x) \,, \tag{130}$$

where

$$x = \frac{0.9 - \alpha_{vap}}{0.9 - 0.6} \,. \tag{131}$$

4.2.5 Transition between Inverted Slug and Dispersed Flow Regimes

The transition between the inverted slug and dispersed flow regimes is determined from the liquid entrainment fraction. In this transition region, part of the liquid phase is considered to be entrained in the dispersed droplet form, and the remaining part is considered to be inverted slugs. The interfacial drag coefficient is modeled with a linear interpolation:

$$C_i = EC_{i,DF} + (1 - E) C_{i,IS} \,, \tag{132}$$

where E is the entrainment fraction. The entrainment fraction is defined as

$$E = \frac{G_d}{G_{liq}} \,, \tag{133}$$

where G_d is the entrained mass flux, and G_{liq} is the magnitude of the liquid phase mass flux. In code implementation, G_{liq} is taken as the larger value between $|\alpha_{liq}\rho_{liq}u_{liq}|$ and 10^{-10}. As suggested in the TRACE manual [3], the entrained mass flux is modeled as

$$G_d = \begin{cases} 0 & j_{vap} \le j_{vap,crit} \\ 2.16 \times 10^{-4} \left[\left(\frac{j_{vap}}{j_{vap,crit}} \right)^3 - 1 \right] N_{\mu g}^{0.236} \Delta\rho j_{vap} & j_{vap} > j_{vap,crit} \end{cases} , \tag{134}$$

where $j_{vap,crit}$ is the critical vapor phase superficial velocity:

$$j_{vap,crit} = 0.6 \left[\frac{\sigma^{0.316} g^{0.228} \Delta\rho^{0.228}}{\rho_{vap}^{0.456} \mu_{vap}^{0.0879}} \right] . \tag{135}$$

The value of the entrainment fraction is also limited to be smaller or equal to 1.

This concludes the interfacial drag model in flow channels for post-CHF flow conditions, including inverted annular, inverted slug, dispersed flow, and transitions between these flow regimes.

5 Interfacial Heat Transfer

When the two phases are under thermal non-equilibrium condition, the temperature difference between the two phase drives heat transfer towards their interface, which consequently leads to mass transfer (in terms of evaporation or condensation) on the interface. Recall that, in the 7-equation model, the interfacial mass transfer term is modeled as

$$\Gamma^{int}_{liq\to vap} A_{int} = \frac{h_{conv,liq} A_{int}(T_{liq} - T_{int}) + h_{conv,vap} A_{int}(T_{vap} - T_{int})}{h_{vap,int} - h_{liq,int}} \,. \tag{136}$$

For two-phase flow, the volumetric heat transfer coefficient, $H_{ik} = h_{conv,k} A_{int}$, is discussed in this chapter for flow regimes of both pre-CHF and post-CHF conditions in this chapter. For convenience, the terms $h_{conv,k} A_{int}$ and $h_{ki} A_i'''$ will be used interchangeably in this chapter.

5.1 Pre-CHF Flow Regimes

In the pre-CHF regimes for vertical pipes, similar to the interfacial drag, the interfacial heat transfer is modeled in the bubbly, cap/slug, annular/mist flow, as well as a transitional regime. The flow regime map for vertical pipes under pre-CHF conditions is shown in Fig. 3.

5.1.1 Bubbly Flow

For the bubbly flow regime, only the dispersed bubbles contribute to the interfacial heat transfer, and thus

$$(h_{li} A_i''')_{Bubbly} = (h_{li} A_i''')_{DB} \,. \tag{137}$$

Here, subscript DB stands for the dispersed bubbly flow. When evaluating interfacial heat transfer, the bubbly flow regime is defined as

$$\alpha_{vap} < \alpha_{vap,DB} \,, \tag{138}$$

where α_{DB} is modeled as

$$\alpha_{vap,DB} = \begin{cases} 0.3 & G \le 2000\,\mathrm{kg/m^2 s} \\ 0.3 + 0.2\left(\frac{G-2000}{2700-2000}\right) & 2000 < G < 2700\,\mathrm{kg/m^2 s} \\ 0.5 & G \ge 2700\,\mathrm{kg/m^2 s} \end{cases} , \tag{139}$$

and G is the total mass flux of the two phases.

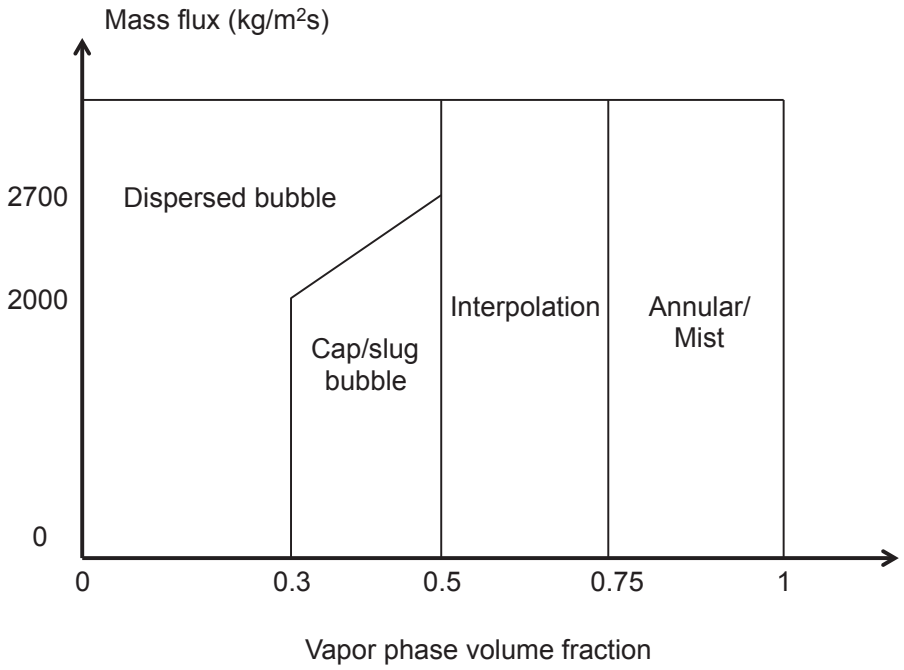

Figure 3. Flow regime map in vertical pipes under the pre-CHF conditions, for interfacial heat transfer [3].

The interfacial area for the dispersed bubbles is simply modeled as

$$A'''_{i,DB} = \frac{6\alpha_{vap}}{d_{DB}}\,, \tag{140}$$

where the diameter of the dispersed bubbles is approximated by

$$d_{DB} = 2\,\mathrm{La} = 2\sqrt{\frac{\sigma}{g\Delta\rho}}\,, \tag{141}$$

where La is the the Laplace coefficient.

According to the TRACE manual [3], this value is constrained in TRACE to lie within the range

$$10^{-4}\,\mathrm{m} \leq d_{DB} \leq 0.9D_h\,, \tag{142}$$

where D_h is the hydraulic diameter of the channel.

For the heat transfer between the liquid and bubble interface, in both evaporation and condensation, the heat transfer coefficient is

$$h_{li,DB} = \frac{k_{liq}}{d_{DB}}\mathrm{Nu}_{DB}\,, \tag{143}$$

where the Nusselt number is given by

$$\mathrm{Nu}_{DB} = 2.0 + 0.6\mathrm{Re}_{DB}^{1/2}\,\mathrm{Pr}_{liq}^{1/3} \tag{144}$$

and Pr_{liq} is the Prandtl number of the liquid phase.

The bubble Reynolds number, Re_{DB}, defined as a function of the dispersed bubble relative velocity, is

$$\mathrm{Re}_{DB} = \frac{\rho_{liq} u_{r,DB} d_{DB}}{\mu_{liq}}\,. \tag{145}$$

The relative velocity between the dispersed bubble and liquid phase is limited to be smaller than its terminal velocity:

$$u_{r,DB} = \min\left(|u_{vap} - u_{liq}|, u_{DB,term}\right)\,. \tag{146}$$

The terminal velocity can be calculated as

$$u_{DB,term} = u_{r,\infty}(1-\alpha_{vap})^{1.39}\,, \tag{147}$$

where $u_{r,\infty}$ is, for a single distorted particle,

$$u_{r,\infty} = \sqrt{2}\left(\frac{\sigma g \Delta\rho}{\rho_{liq}^2}\right)^{1/4}\,. \tag{148}$$

The heat transfer between the vapor and bubble interface is simplified by using a constant value

$$h_{vi} = 1000\,\mathrm{W/m^2K}\,. \tag{149}$$

5.1.2 Cap Bubble/Slug Flow

For the cap bubble/slug flow regime, defined by the boundary $\alpha_{vap,DB} \leq \alpha \leq 0.5$, the interfacial heat transfer consists of contributions of both small dispersed bubbles and of large bubbles:

$$(h_{li}A_i''')_{CS} = (h_{li}A_i''')_{DB} + (h_{li}A_i''')_{LB}\,, \tag{150}$$

where subscripts CS and LB denote cap/slug flow and large bubble, respectively. For the small dispersed bubbles, the heat transfer coefficient between the liquid and the bubble interface is calculated the same way as in the bubbly flow regime. However, in the cap bubble/slug flow regime, the interfacial area for the small dispersed bubbles are calculated differently:

$$A_{i,DB}''' = \frac{6\alpha_{vap,DB}}{d_{DB}}\left(\frac{1-\alpha_{vap}}{1-\alpha_{vap,DB}}\right)\,. \tag{151}$$

The interfacial area associated with the large bubbles is computed as

$$A'''_{i,LB} = \frac{C^*}{D^*}\left(\frac{\alpha_{vap} - \alpha_{vap,DB}}{1 - \alpha_{vap,DB}}\right) . \tag{152}$$

Here the coefficient C^* and the diameter D^* depend on the channel hydraulic diameters:

$$C^* = \begin{cases} 4.5; & D_h < D_{h,crit} \\ 16; & D_h \geq D_{h,crit} \end{cases} , \tag{153}$$

and

$$D^* = \begin{cases} D_h; & D_h < D_{h,crit} \\ D_{h,crit}; & D_h \geq D_{h,crit} \end{cases} , \tag{154}$$

where $D_{h,crit} = 50\mathrm{La}$, defined in Equation (114).

For these large bubbles, the heat transfer coefficient between the liquid and the bubble interface is calculated as

$$h_{li,LB} = \frac{k_{liq}}{D^*}\mathrm{Nu}_{LB} , \tag{155}$$

where the Nusselt number, Nu_{LB}, is calculated using Equation (144), with a modified bubble Reynolds number that is defined as

$$\mathrm{Re}_{LB} = \frac{\rho_{liq} u_{r,LB} D^*}{\mu_{liq}} . \tag{156}$$

The relative velocity of the large bubbles is defined as

$$u_{r,LB} = \min\left(|u_{vap} - u_{liq}|, u_{LB,term}\right) , \tag{157}$$

and the terminal velocity for the large bubbles are calculated as

$$u_{LB,term} = \begin{cases} u_{r,\infty} & d^*_{LB} < 0.125 \\ 1.13 u_{r,\infty} e^{-d^*_{LB}} & 0.125 \leq d^*_{LB} < 0.6 \\ \frac{0.496 u_{r,\infty}}{\sqrt{d^*_{LB}}} & d^*_{LB} \geq 0.6 \end{cases} . \tag{158}$$

Here the non-dimensional bubble diameter is defined as

$$d^*_{LB} = \frac{D^*}{D_h} , \tag{159}$$

and a relative velocity in an infinite medium is given by

$$u_{r,\infty} = \frac{\sqrt{2}}{2}\frac{\sqrt{g\Delta\rho D^*}}{\rho_{liq}} . \tag{160}$$

For the cap bubble/slug flow regime, the heat transfer between the vapor and the bubble interface are calculated similarly to that from the liquid phase to the bubble interface:

$$(h_{vi} A'''_i) = h_{vi}(A'''_{i,DB} + A'''_{i,LB}) , \tag{161}$$

and the same constant value of $1000\,\mathrm{W/m^2K}$ is used for h_{vi}.

5.1.3 Correction for Subcooled Boiling

When subooled boiling is present, TRACE code [3] recommends a correction factor for the volumetric heat transfer coefficient of the liquid phase for the dispersed bubble part. The subcooled boiling condition is determined by the following two conditions:

$$\Gamma^{wall}_{liq\rightarrow vap} > 0\,, \tag{162}$$

and

$$T_{liq} < T_{sat}\,. \tag{163}$$

Here, T_{sat} is set to be T_{int}. Under subcooled boiling condition, the volumetric heat transfer coefficient of the liquid phase for the dispersed bubble part is given by

$$(h_{li}A'''_i)_{DB} = (1 - wf_{SB})(h_{li}A'''_i)_{DB} + wf_{SB}(h_{li}A'''_i)_{SB}\,, \tag{164}$$

in which $(h_{li}A'''_i)_{SB}$ is modeled as

$$(h_{li}A'''_i)_{SB} = 0.075 h_{fg}\frac{\rho_{liq}\rho_{vap}}{\Delta\rho}\max(10^{-4}, \alpha_{vap})\,. \tag{165}$$

The subcooled boiling weighting factor is defined as

$$wf_{SB} = \max\left\{0, \min[1, 10(0.2 - \alpha_{vap})]\right\}\,. \tag{166}$$

Note that such a correction factor is not applied to the vapor phase.

5.1.4 Annular/Mist Flow

For the annular/mist flow regime, the interfacial heat transfer consists of the sum of two components, corresponding to the annular liquid film and entrained liquid droplets

$$(h_{li}A'''_i)_{AM} = (h_{li}A'''_i)_{film} + (h_{li}A'''_i)_{drops}\,. \tag{167}$$

At first, the film thickness is computed as

$$\delta = \frac{D_h}{2}\left(1 - \sqrt{\alpha_{vap}}\right)\,, \tag{168}$$

and this value is limited to be greater than 10 μm. The interfacial area associated with the liquid film is calculated as a function of the volume fraction of the vapor phase and hydraulic diameter:

$$A'''_i = \frac{4}{D_h}\sqrt{\alpha_{vap}}\,. \tag{169}$$

For a special case where the surface is considered to be partially wetted by the liquid film, the interfacial area is modified to consider the partially wetted condition, such that

$$A_i''' = \frac{4}{D_h}\sqrt{\alpha_{vap}} f_{wet}\,, \tag{170}$$

where the fraction of the surface wetted by the liquid film, f_{wet}, is estimated by

$$f_{wet} = \frac{(1-\alpha_{vap})D_h}{4(25\times 10^{-6})}\,. \tag{171}$$

The surface is considered to be partially wetted when the liquid film thickness reaches the minimum critical value, 25 μm.

The liquid-film-to-interface heat transfer, $h_{li,film}$, is modeled by using a power-law weighting of the turbulent and laminar regimes:

$$h_{li,film} = \left(h_{li,film,lam}^2 + h_{li,film,turb}^2\right)^{1/2}\,. \tag{172}$$

The correlation for the laminar regime is based on the well known Kuhn-Schroch-Peterson correlation:

$$\mathrm{Nu}_{li,film,lam} = 2(1 + 1.83\times 10^{-4}\mathrm{Re}_f)\,, \tag{173}$$

where the film Reynolds number is calculated as

$$\mathrm{Re}_f = \frac{G_{liq}D_h}{\mu_{liq}}\,, \tag{174}$$

and G_{liq} is the liquid phase mass flux. For the turbulent regime,the Gnielinski correlation is used with a multiplier:

$$\mathrm{Nu}_{li,film,turb} = 0.7\mathrm{Nu}_{Gnielinski}\,. \tag{175}$$

The Gnielinski correlation will be discussed in the wall heat transfer section. For both the laminar and turbulent regimes, the heat transfer coefficient is related to the Nusselt number using the film thickness as reference length scale:

$$\mathrm{Nu}_{li,film,lam/turb} = \frac{h_{li,film,lam/turb}\delta}{k_{liq}}\,. \tag{176}$$

For the liquid film part, the vapor-core-to-liquid-film-interface heat transfer coefficient is modeled as

$$h_{vi,film} = \frac{k_{vap}}{D_c}\mathrm{Nu}_{vi}\,, \tag{177}$$

where D_c is the diameter of the annular vapor core approximated by

$$D_c \approx \sqrt{\alpha_{vap}} D_h\,. \tag{178}$$

The vapor-interface Nusselt number is modeled by the Dittus-Boelter correlation, and is limited to be larger than 4:

$$\mathrm{Nu}_{vi} = \max\{4, 0.23\mathrm{Re}_c^{0.8} \underset{vap}{\overset{0.4}{\mathrm{Pr}}}\}\,, \tag{179}$$

where the Reynolds number for the annular vapor core is calculated as

$$\mathrm{Re}_c = \frac{G_{vap} D_c}{\mu_{vap}}\,, \tag{180}$$

and G_{vap} is the mass flux of the vapor phase, and Pr_{vap} is the Prandtl number of the vapor phase.

For the droplets, the volumetric interfacial area density is modeled as

$$A'''_{i,drop} = \frac{6\alpha_{vap}\alpha_d}{(1-\alpha_d)d_d}\,, \tag{181}$$

for which α_d is the fraction of the annular core region occupied by the droplets, and d_d is the droplet size. Both of these two quantities have been discussed in the interfacial drag model section, in Equations (93) and (95), respectively.

The liquid-to-interface heat transfer coefficient for the droplets is modeled as

$$h_{li,drop} = 2\pi^2 \frac{k_{liq}}{d_d}\,. \tag{182}$$

The vapor-to-interface heat transfer coefficient for the droplets part is modeled as

$$h_{vi,drop} = \frac{\mathrm{Nu}_{vi,drop} d_d}{k_{vap}}\,, \tag{183}$$

where $\mathrm{Nu}_{vi,drop}$ is the Nusselt number, modeled as

$$\mathrm{Nu}_{vi,drop} = 2 + \sqrt{u^*_{max}\mathrm{Pé}}\,, \tag{184}$$

where u^*_{max} is the maximum dimensionless circulation velocity at the surface of the drop. Here Pé is the droplet Peclet number, defined by

$$\mathrm{Pé} \equiv \frac{\rho_{vap} c_{p,vap} d_d u_r}{k_{vap}}\,, \tag{185}$$

where u_r is the drop relative velocity, defined as

$$u_r = 2.462\sqrt{\frac{g\Delta\rho d_d}{2\rho_{vap}}}\,. \tag{186}$$

The maximum dimensionless circulation velocity at the surface of the droplet, u^*_{max}, is defined as

$$u^*_{max} = \frac{1.5}{1 + \frac{2.8(1+2\lambda)(2+3\kappa)}{(2+3\lambda)\sqrt{\mathrm{Re}_d}}}\,, \tag{187}$$

where

$$\mathrm{Re}_d = \frac{\rho_{vap} u_r d_d}{\mu_{vap}}\,, \tag{188}$$

$$\lambda = \sqrt{\frac{\rho_{liq}\mu_{liq}}{\rho_{vap}\mu_{vap}}}\,, \tag{189}$$

and

$$\kappa = \frac{\mu_{liq}}{\mu_{vap}}\,. \tag{190}$$

The drop Reynolds number, Re_d, is limited to be in the range $0.5 \le \mathrm{Re}_d \le 200$. The maximum dimensionless circulation velocity at the surface of the drop, u^*_{max}, is limited to be in the range $0.0001 \le u^*_{max} \le 1.0$.

5.1.5 Transition between Bubbly/Slug and Annular/Mist Flow

For the transition region, i.e., $0.5 \le \alpha_{vap} \le 0.75$, a simple linear interpolation is used to determine the interfacial heat transfer coefficients:

$$(h_{ki}A'''_i) = wf_{AM}(h_{ki}A'''_i)_{AM} + (1 - wf_{AM})(h_{ki}A'''_i)_{BS}\,, \tag{191}$$

where the weighting factor is defined by

$$wf_{AM} = \frac{\alpha_{vap} - 0.5}{0.75 - 0.5}\,. \tag{192}$$

The value of $(h_{ki}A'''_i)_{AM}$ is calculated using the annular/mist flow regime model. The value of $(h_{ki}A'''_i)_{BS}$ is calculated using either the dispersed bubble flow regime model or the cap/slug model, depending on the two-phase flow mass flux (see Figure 3).

5.1.6 Horizontal Stratified Flow

When the flow is considered to be horizontal stratified flow, the volumetric interfacial heat transfer coefficients are calculated as

$$(h_{ki}A'''_i)_{strat} = h_{ki,strat}A'''_{i,strat}\,. \tag{193}$$

The interfacial area density, $A'''_{i,strat}$, is obtained as

$$A'''_{i,strat} = \frac{S_{int}}{A}\,, \tag{194}$$

with S_{int} being the width of the stratified two-phase interface; see Equation (39) and Figure 1. The liquid side interfacial heat transfer coefficient is modeled as

$$h_{li,strat} = \frac{k_{liq}}{h_{liq}} Nu_{li}\,, \tag{195}$$

where h_{liq} is the liquid level, see Equation (41) and Figure 1. The Nusselt number, Nu_{li}, for the liquid phase interfacial heat transfer coefficient is calculated the same way as it is calculated for the annular/mist flow regime, namely, Equations (172), (173), and (175). The liquid phase Reynolds number used in these equations is the same as defined in Equation (34). Following TRACE code suggestion [3], the final value of $h_{li,strat}$ is limited to be smaller than 2.5×10^4.

For the vapor phase, the volumetric interfacial heat transfer coefficient is simply calculated as

$$(h_{vi}A'''_i)_{strat} = 1000 A'''_{i,strat}\,. \tag{196}$$

5.1.7 Transition between Stratified and Non-Stratified Flow

If the flow regime is considered to be in a transition between stratified and non-stratified condition, a power law based interpolation is used:

$$(h_{ki}A'''_i) = (h_{ki}A'''_i)^n_{strat}(h_{ki}A'''_i)^{(1-n)}_{non-strat}\,, \tag{197}$$

where subscripts $strat$ and $non-strat$ represent for stratified flow and non-stratified flow conditions, respectively. The exponent, n, is set equal to wf_{strat}, given by Equation (47).

This concludes the interfacial heat transfer model for pre-CHF flow regimes.

5.2 Post-CHF Flow Regimes

For post-CHF flow regimes, interfacial heat transfer coefficients must be defined in the following flow regimes: inverted annular, inverted slug, dispersed flow regimes, and transition regimes between them. The flow regime map for post-CHF interfacial heat transfer is the same as shown in Figure 2.

5.2.1 Inverted Annular Flow

Under post-CHF condition, if the void fraction is smaller than 0.6, the flow is treated as inverted annular flow. Assuming that the liquid core takes a cylindrical shape, its diameter can be obtained as

$$D_c = \sqrt{1-\alpha_{vap}} D_h \,, \tag{198}$$

and the interfacial area can be obtained as

$$A_i''' = \sqrt{1-\alpha_{vap}} \frac{4}{D_h} \,. \tag{199}$$

If the liquid core is in subcooled condition, following the TRACE code [3], the liquid phase interfacial heat transfer coefficient is simply calculated as

$$h_{li} = \frac{\mathrm{Nu}_{li} k_{liq}}{D_c} \,, \tag{200}$$

with Nu_{li} = 100. If the liquid core is in superheated condition, a correction factor for superheating condition is used, and the liquid phase interfacial heat transfer coefficient is corrected as

$$h_{li} = h_{li} \left[1 + \Delta T_{sup}(250 + 50\Delta T_{sup})\right] \,, \tag{201}$$

where ΔT_{sup} is the liquid superheat.

For the vapor phase interfacial heat transfer coefficient, the vapor film thickness, δ, has to be determined first from Equation (111) for tube geometry, and Equation (112) for rod bundle geometry. Following the TRACE code [5], the vapor phase interfacial heat transfer coefficient is then calculated as

$$h_{vi} = 2\frac{k_{vap}}{\delta} \,. \tag{202}$$

5.2.2 Inverted Slug and Dispersed Flow

Under post-CHF condition, if the void fraction is larger than 0.9, the flow is treated as inverted slug flow, dispersed flow, or a transition regime between them, which depends on the liquid entrainment fraction. Thus, the interfacial heat transfer coefficients in these regimes are modeled as

$$(h_{ki} A_i''') = (1-E)(h_{ki} A_i''')_{IS} + E(h_{ki} A_i''')_{DF} \,, \tag{203}$$

where subscripts IS and DF denote inverted slug and dispersed flow conditions, respectively.

For dispersed flow condition, the interfacial area density is modeled as

$$A_i''' = \frac{6(1-\alpha_{vap})}{d_{SM}}\,, \tag{204}$$

where d_{SM} is the droplet Sauter mean diameter, which has been discussed in the previous section, i.e., Equation (118). For the liquid phase interfacial heat transfer coefficient, the same correlation for annular/mist flow droplet filed is used, i.e., Equation (182) with d_d replaced by d_{SM}. Again, the liquid phase superheated condition needs to be considered, similar to the inverted annular flow condition. Putting this together, the liquid phase interfacial heat transfer coefficient becomes

$$h_{li} = 2\pi^2 \frac{k_{liq}}{d_{SM}} \left[1 + \Delta T_{sup}(250 + 50\Delta T_{sup})\right]\,. \tag{205}$$

The vapor phase interfacial heat transfer coefficient is modeled as

$$h_{vi} = \frac{k_{vap}}{d_{SM}} \mathrm{Nu}_d\,, \tag{206}$$

with Nu_d being the droplet Nussult number. Following TRACE code suggestion [3], Nu_d is modeled as

$$\mathrm{Nu}_d = \frac{2 + 0.57\mathrm{Re}_d^{1/2}\,\mathrm{Pr}_{vap}^{1/3}}{(1+B_f)^{0.7}}\,. \tag{207}$$

The droplet Reynolds number, Re_d, is defined as

$$\mathrm{Re}_d = \frac{\rho_{vap} V_r d_{SM}}{\mu_{vap}}\,, \tag{208}$$

with

$$V_r = \min\left[|u_{vap} - u_{liq}|, V_\infty \alpha_{vap}^{1.4}\right]\,. \tag{209}$$

The single-particle terminal velocity, V_∞, is modeled as

$$V_\infty = 0.6 \frac{\sigma^{0.316}(g\Delta\rho)^{0.228}}{\rho_{vap}^{0.456}\mu_{vap}^{0.0879}}\,. \tag{210}$$

Following the TRACE code [3], the blowing factor is simply approximated as

$$B_f = \frac{h_{vap} - h_{vap,sat}}{h_{fg}}\,. \tag{211}$$

For inverted slug flow, the interfacial area density is calculated as

$$A_i''' = \frac{4.8104(1-\alpha_{vap})}{d_{IS}}\,, \tag{212}$$

where d_{IS} is the diameter of the ligament, with subscript IS denoting inverted slug flow condition. Following the TRACE code [3], d_{IS} is approximated as

$$d_{IS} = 0.6325 D_h \,. \tag{213}$$

The liquid phase interfacial heat transfer coefficient is modeled in a two-step manner. First, it is calculated the same way as it is done for the dispersed flow, i.e., Equation (205) with d_{SM} replaced by d_{IS}. Second, the coefficient is corrected with an enhancement factor:

$$h_{li} = h_{li,1} 4 \min \left[1, \left(\frac{d_{IS}}{d_{RT}} \right)^2 \right] \,, \tag{214}$$

in which $h_{li,1}$ is the interfacial heat transfer coefficient calculated from the first step. Following the TRACE code [3], the Sauter mean diameter for a distribution having a maximum diameter that is stable against the Rayleigh-Taylor instability, d_{RT}, is modeled as

$$d_{RT} = \frac{3.52}{4} \sqrt{\frac{\sigma}{g \Delta \rho}} \tag{215}$$

For the vapor phase interfacial heat transfer coefficient, the same model used in the dispersed flow regime is used, i.e., Equation (206). Note that, in both Equations (206) and (208), d_{SM} is replaced by d_{IS}.

5.2.3 Interpolation Region

For interpolation region, which is defined between void fraction 0.6 and 0.9, linear interpolation is used to obtain interfacial heat transfer coefficients

$$(h_{ki} A_i''') = w f_{IA} (h_{ki} A_i''')_{IA} + (1 - w f_{IA}) (h_{ki} A_i''')_{IS-DF} \tag{216}$$

in which subscripts IA and $IS - DF$ denote inverted annular and inverted slug-dispersed flow conditions, respectively. Recall that, $(h_{ki} A_i''')_{IS-DF}$ is calculated as entrainment fraction weighted function of inverted slug and dispersed flow interfacial heat transfer coefficients, i.e., Equation (203). The final expression for the interpolation region is

$$(h_{ki} A_i''') = w f_{IA} (h_{ki} A_i''')_{IA} + (1 - w f_{IA}) \left[(1 - E)(h_{ki} A_i''')_{IS} + E (h_{ki} A_i''')_{DF} \right] \,. \tag{217}$$

The weighting function, $w f_{IA}$, is modeled as

$$w f_{IA} = 2 x_{IA} - x_{IA}^2 \,, \tag{218}$$

with

$$x_{IA} = \frac{0.9 - \alpha_{vap}}{0.9 - 0.6} \,. \tag{219}$$

This concludes the interfacial heat transfer coefficients for post-CHF regimes, including inverted annular, inverted slug, dispersed flow, and transitional regions between them.

6 Wall Heat Transfer

For the 7-equation two-phase flow model presented in Section 2, the wall heat transfer model is required both in the determination of the heat transferred from solid surfaces, and also the rate of vapor phase generation occurring near those surfaces. Currently, a simplified heat flux partitioning model is used to determine the mass transfer associated with wall boiling

$$Q^{boil}_{wall,liq} = (1-\beta)h_{wall,liq}(T_{wall} - T_{liq})\kappa\,, \tag{220}$$

$$Q^{conv}_{wall,liq} = \beta h_{wall,liq}(T_{wall} - T_{liq})\kappa\,, \tag{221}$$

$$Q_{wall,vap} = h_{wall,vap}(T_{wall} - T_{vap})(1-\kappa)\,, \tag{222}$$

and the total wall heat flux balance is given as

$$Q_{wall,total} = Q^{boil}_{wall,liq} + Q^{conv}_{wall,liq} + Q_{wall,vap}\,. \tag{223}$$

The wall boiling mass transfer is then determined as

$$\Gamma^{wall}_{liq\to vap} = \frac{Q^{boil}_{wall,liq}}{\left[e_{vap,sat}(\bar{p}_{int}) + \frac{\bar{p}_{int}}{\rho_{vap,sat}(\bar{p}_{int})}\right] - h_{liq}(\rho_{liq}, e_{liq})}\,. \tag{224}$$

The main purpose of this section is to describe the phasic heat transfer coefficient $h_{wall,k}$ (or in short $h_{w,k}$) for both the pre-CHF and post-CHF conditions. More details on wall heat flux partitionings (parameters β and κ) can be found in Section 3.2 of the RELAP-7 theory manual [4].

6.1 Pre-CHF Wall Heat Transfer

For pre-CHF wall heat transfer, the logic to determine which heat transfer mode is shown in Figure 4.

6.1.1 Single-Phase Liquid Flow

For single-phase liquid flow condition, the wall heat transfer coefficient, $h_{w,liq}$, is taken to be the maximum value of laminar flow, turbulent flow, and natural circulation condition:

$$h_{w,liq} = \max\left\{h_{lam}, h_{turb}, h_{NC}\right\}\,, \tag{225}$$

in which the subscripts lam, $turb$, and NC stand for laminar flow, turbulent flow, and natural circulation flow conditions, respectively. They are discussed for both the tube and rod bundle geometries.

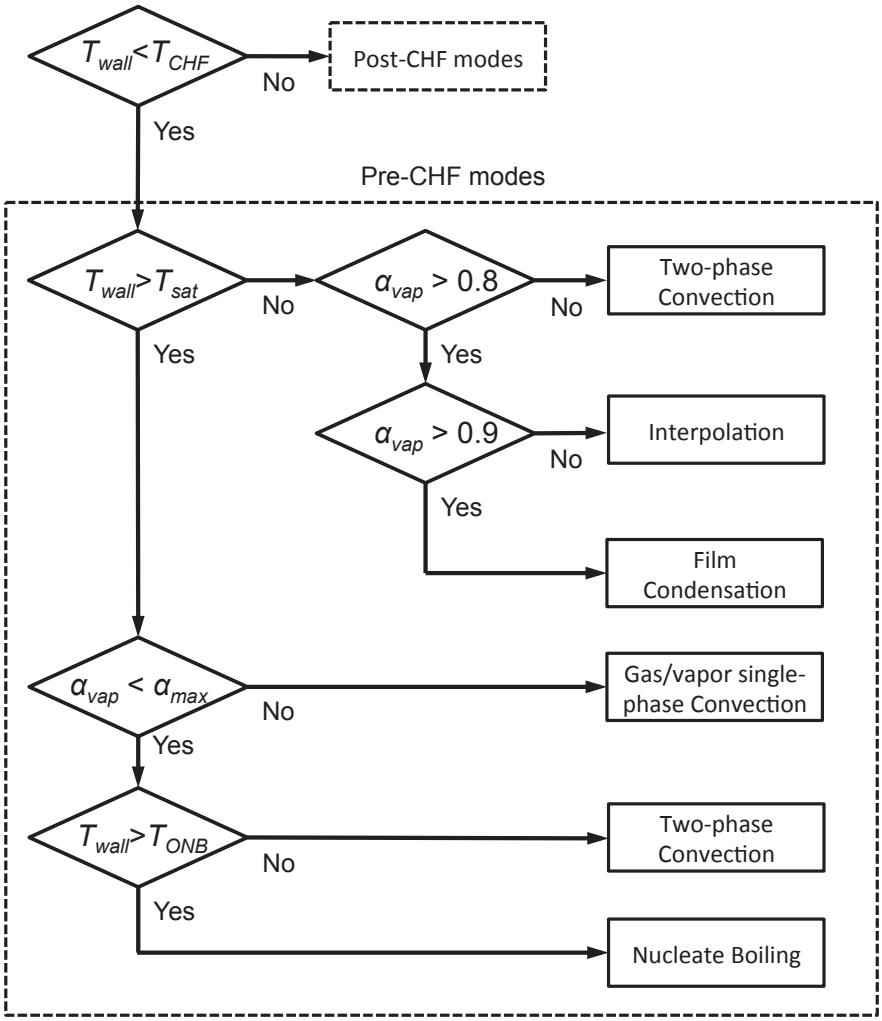

Figure 4. Logic to determine pre-CHF wall heat transfer mode following TRACE code [3].

6.1.1.1 Tube Geometry

For tube geometry, the laminar flow heat transfer coefficient is calculated as

$$h_{lam} = \mathrm{Nu}_{lam} \frac{k_{liq}}{D_h} \,, \tag{226}$$

in which Nu_{lam} is a constant. $\mathrm{Nu}_{lam} = 4.36$ for constant wall heat flux condition, and $\mathrm{Nu}_{lam} = 3.66$ for constant wall temperature condition.

For tube geometry, following the TRACE code [3], the turbulent flow heat transfer coefficient is modeled with the Gnielinski correlation and corrected by a temperature factor. The Gnielinski correlation is given by

$$\mathrm{Nu}_{Gnielinski} = \frac{(f/2)(\mathrm{Re} - 1000)\,\mathrm{Pr}}{1 + 12.7(f/2)^{1/2}\left(\mathrm{Pr}^{2/3} - 1\right)} \,, \tag{227}$$

where the friction factor, f, is given as

$$f = \left[1.58\ln(\mathrm{Re}) - 3.28\right]^{-2} \tag{228}$$

Under single-phase liquid flow condition, the corresponding Reynolds number is defined as

$$\mathrm{Re}_{liq} = \frac{\rho_{liq} u D_h}{\mu_{liq}} \tag{229}$$

and is limited to be larger than 1000. The Nusselt number obtained from Equation (227) is then corrected with a correction factor as

$$\mathrm{Nu}_{turb} = \mathrm{Nu}_{Gnielinski} \left(\frac{\mathrm{Pr}_{liq}}{\mathrm{Pr}_w}\right)^{0.11} \,, \tag{230}$$

in which Pr_{liq} is the Prandtl number evaluated with liquid phase temperature, and Pr_w is the Prandtl number evaluated with wall temperature. The value of $\mathrm{Pr}_{liq} \,/\, \mathrm{Pr}_w$ is limited in the range of [0.05, 20].

For tube geometry, following the TRACE code [3], the natural circulation heat transfer coefficient is taken as the larger one between the laminar flow and turbulent flow conditions:

$$\mathrm{Nu}_{NC} = \max\left(\mathrm{Nu}_{NC,lam}, \mathrm{Nu}_{NC,turb}\right) \,, \tag{231}$$

with

$$\mathrm{Nu}_{NC,lam} = 0.59 \left(\mathrm{Gr}_{liq} \underset{liq}{\mathrm{Pr}}\right)^{1/4} \,, \tag{232}$$

and

$$\mathrm{Nu}_{NC,turb} = 0.13 \left(\mathrm{Gr}_{liq} \underset{liq}{\mathrm{Pr}}\right)^{1/3} \,. \tag{233}$$

In both equations, the liquid phase Grashof number is defined as

$$\mathrm{Gr}_{liq} = \frac{g\beta_{liq}\Delta T D_h^3}{\left(\mu_{liq}/\rho_{liq,film}\right)^2}\,, \tag{234}$$

where

$$\Delta T = |T_w - T_{liq}|\,, \tag{235}$$

and $\rho_{liq,film}$ is the liquid density evaluated from the $film$ temperature:

$$T_{film} = 0.5(T_w + T_{liq})\,. \tag{236}$$

6.1.1.2 Rod Bundle Geometry

For rod bundle geometry, the laminar flow wall heat transfer coefficient is taken as the larger one between the value by the El-Genk laminar formula and the value by the Kim & Li formula [3]:

$$h_{lam} = \max\left(h_{EG,lam}, h_{KL,lam}\right)\,, \tag{237}$$

where the subscripts EG and KL denote the El-Genk laminar formula and Kim & Li formula, respectively. The El-Genk laminar formula is given by

$$\mathrm{Nu}_{EG,lam} = A\mathrm{Re}^B\,\mathrm{Pr}^{0.33}\,, \tag{238}$$

where

$$\begin{aligned} A &= 2.97 - 1.76(P/D_r) \\ B &= 0.56(P/D_r) - 0.30 \end{aligned}\,. \tag{239}$$

Following the TRACE code [3], a curve-fitted formula is given to represent the Kim & Li tabular data:

$$\mathrm{Nu}_{KL,lam} = -5.6605\left(\frac{P}{D_r}\right)^2 + 31.061\left(\frac{P}{D_r}\right) - 24.473\,. \tag{240}$$

In both equations, P/D_r is the pitch-to-diameter ratio for the rod bundle geometry.

For rod bundle geometry, the turbulent flow wall heat transfer coefficient is modeled using the El-Genk turbulent formula, and then corrected by taking into consideration the wall temperature effect. The El-Genk turbulent correlation is given by

$$Nu_{EG,turb} = C_{EG}Re^{0.8}Pr^{0.33}\,, \tag{241}$$

where

$$C_{EG} = 0.028\left(\frac{P}{D_r}\right) - 0.006\,. \tag{242}$$

Again, P/D_r is the pitch-to-diameter ratio. The wall temperature effect is then considered, and the final form becomes

$$\mathrm{Nu}_{turb} = \mathrm{Nu}_{EG,turb} \left(\frac{\mathrm{Pr}_{liq}}{\mathrm{Pr}_w} \right)^{0.11} , \tag{243}$$

with $\mathrm{Pr}_{liq} \,/\, \mathrm{Pr}_w$ limited in the range of [0.05, 20].

For rod bundle geometry, the natural circulation wall heat transfer coefficient is modeled with the Sarma's formulation, as suggested by the TRACE code [3]

$$\mathrm{Nu}_{NC} = 0.7 \left(\mathrm{Gr}_D \underset{liq}{\mathrm{Pr}} \right)^{1/4} \tag{244}$$

where the Grashof number is defined the same as Equation (234), and the same wall temperature effect is considered.

6.1.2 Two-Phase Forced Convection

Following TRACE code suggestion [3], with respect to single-phase forced convection flow condition, the primary role of two-phase forced convection enhancement is to correct the liquid Reynolds number. Thus, for two-phase forced convection flow condition, the same single-phase forced convection formulas are used, with a modified liquid phase Reynolds number:

$$\mathrm{Re}_{2\Phi} = \frac{\rho_{liq} u_{liq} D_h}{\mu_{liq}} \tag{245}$$

Note that, under two-phase forced convection condition, the wall heat transfer coefficient is applied to the liquid phase only, and thus, $h_{w,vap} = 0$.

6.1.3 Film Condensation

For film condensation condition, the wall heat transfer is assumed to take place between the wall and the liquid phase, and

$$h_{w,liq} = \frac{k_{liq}}{\delta} \mathrm{Nu}_{w,liq} \,, \tag{246}$$

in which δ is the film thickness, given by

$$\delta = \frac{D_h}{2} (1 - \sqrt{\alpha_{vap}}) \tag{247}$$

and is limited to be greater than 10 μm.

The Nusselt number, $\mathrm{Nu}_{w,liq}$, is computed using a power-law-based weighting function as

$$\mathrm{Nu}_{w,liq} = \left(\mathrm{Nu}_{lam}^2 + \mathrm{Nu}_{turb}^2\right)^{1/2} , \tag{248}$$

where the subscripts lam and $turb$ denote laminar flow and turbulent flow conditions, respectively. Following the TRACE code suggestion [3], the Kuhn-Shrock-Peterson (K-S-P) correlation is used for the laminar flow condition:

$$\mathrm{Nu}_{lam} = 2\left(1 + 1.83 \times 10^{-4}\mathrm{Re}_f\right) , \tag{249}$$

with Re_f defined as

$$\mathrm{Re}_f = \frac{\alpha_{liq}\rho_{liq}u_{liq}D_h}{\mu_{liq}} . \tag{250}$$

For turbulent flow condition, the El-Genk correlation, Equation (241), is used, with a $1/4$ correction factor:

$$\mathrm{Nu}_{turb} = \frac{1}{4}\mathrm{Nu}_{EG,turb} . \tag{251}$$

The same liquid phase Reynolds number, Re_f, is used in the El-Genk correlation. Again, for vapor phase, the wall heat transfer coefficient is taken as zero, $h_{w,vap} = 0$.

6.1.4 Transition between Two-Phase Forced Convection and Film Condensation

As shown in Figure 4, for void fractions between 0.8 and 0.9, a linear interpolation is used between the two-phase forced convection value and the film condensation value:

$$h_{w,liq} = wf_{ann}h_{ann} + (1 - wf_{ann})h_{2\Phi} , \tag{252}$$

in which h_{ann} is the film condensation wall heat transfer coefficient, and $h_{2\Phi}$ is the two-phase forced convection wall heat transfer coefficient. The weighting factor, wf_{ann} is defined as

$$wf_{ann} = \frac{\alpha_{vap} - 0.8}{0.9 - 0.8} . \tag{253}$$

6.1.5 Wall Boiling Heat Transfer

For pre-CHF condition, when wall temperature exceeds the onset-of-nucleate-boiling temperature (T_{ONB}), the wall heat transfer mode becomes subcooled nucleate boiling or nucleate boiling, depending on the liquid phase temperature. In RELAP-7, the wall heat transfer for both modes are modeled the same.

6.1.5.1 Onset of Nucleate Boiling

The onset-of-nucleate-boiling temperature is first discussed. Following the TRACE code [3], the wall temperature for onset of nucleate boiling is modeled as

$$T_{ONB} = T_{liq} + \frac{1}{4}\left(\sqrt{\Delta T_{ONB,sat}} + \sqrt{\Delta T_{ONB,sat} + 4\Delta T_{sub}}\right)^2 , \tag{254}$$

in which ΔT_{sub} is the liquid phase subcooling temperature:

$$\Delta T_{sub} = T_{sat} - T_{liq} , \tag{255}$$

and $\Delta T_{ONB,sat}$ is the wall superheat necessary for the onset of nucleate boiling when the liquid is at saturation temperature, defined as

$$\Delta T_{ONB,sat} = \frac{2h_{FC}\sigma T_{sat}}{F^2(\phi)\rho_{vap}h_{fg}k_{liq}} . \tag{256}$$

In this equation, h_{FC} is the two-phase flow forced convection wall heat transfer coefficient; $F(\phi)$ is the contact angle correction factor:

$$F(\phi) = 1 - exp(-\phi^3 - 0.5\phi) . \tag{257}$$

Following the TRACE code [3], a constant value of 38 degrees is taken for the contact angle.

6.1.5.2 Nucleate Boiling Heat Transfer

For both subcooled nucleate boiling and nucleate boiling conditions, the wall heat flux is modeled the same:

$$q''_{NB} = \left[(q''_{FC})^3 + (q''_{PB} - q''_{BI})^3\right]^{1/3} , \tag{258}$$

in which q''_{FC} is the forced convection wall heat flux component:

$$q''_{FC} = h_{FC}(T_{wall} - T_{liq}) , \tag{259}$$

q''_{PB} is the pool boiling wall heat flux component based on wall temperature, and q''_{BI} is the pool boiling wall heat flux component at boiling initiation, based on T_{ONB}. Following the TRACE code [3], the Gorenflo correlation is used to model pool boiling wall heat flux:

$$q''_{PB} = \left[\frac{h_0 F_P}{(q''_0)^n}\right]^{\frac{1}{1-n}} (T_{wall} - T_{sat})^{\frac{1}{1-n}} , \tag{260}$$

with $h_0 = 5600\,\mathrm{W/m^2 - K}$ and $q''_0 = 20000\,\mathrm{W/m^2}$, and

$$n = 0.9 - 0.3P_r^{0.15} . \tag{261}$$

F_P is pressure dependent and is given as a function of the reduced pressure, P_r:

$$F_P = 1.73 P_r^{0.27} + \left(6.1 + \frac{0.68}{1 - P_r}\right) P_r^2 \,, \tag{262}$$

with P_r defined as

$$P_r = \frac{P}{P_{crit}} \,, \tag{263}$$

and P_{crit} is the critical pressure.

6.2 Post-CHF Wall Heat Transfer

For post-CHF conditions, where wall temperature exceeds the CHF wall temperature, post-CHF wall heat transfer modes are used, which include inverted annular film boiling, dispersed flow boiling, a transition between these two boiling conditions, and a transition boiling mode. The logic of post-CHF wall heat transfer modes is shown in Figure 5.

6.2.1 Inverted Annular Film Boiling

Under post-CHF condition, inverted annular film boiling is assumed to take place for void fractions smaller than 0.6. For inverted annular film boiling condition, following the TRACE discussion [3], the wall-to-liquid-phase heat transfer is approximated to have two components, as one being convective heat transfer component, and the other one being radiative heat transfer component. The convective heat transfer component is simplified from the complex wall-to-vapor-phase and vapor-to-interface heat transfer relations. Following the TRACE code, it is modeled as

$$h_{wall,liq,\Gamma} = \frac{k_{vap}}{\delta} \mathrm{Nu}_{wall,liq} \frac{T_{wall} - T_{sat}}{T_{wall} - T_{liq}} \,, \tag{264}$$

in which δ is the vapor film thickness, already discussed in the interfacial drag section. For tube geometry, Equation (111) is used, and for rod bundle geometry, Equation (112) is used. For tube geometry, the Nusselt number is modeled as

$$\mathrm{Nu}_{wall,liq} = \max\left[0, 0.268(\delta^*)^{0.77} - 0.34\right] \,, \tag{265}$$

and for rod bundle geometry, this number is increased with a 30% enhancement:

$$\mathrm{Nu}_{wall,liq} = \max\left\{0, 1.3\left[0.268(\delta^*)^{0.77} - 0.34\right]\right\} \,. \tag{266}$$

The non-dimensional film thickness is given by

$$\delta^* = \delta \left(\frac{\rho_{vap} g \Delta\rho}{\mu_{vap}^2}\right)^{1/3} \,, \tag{267}$$

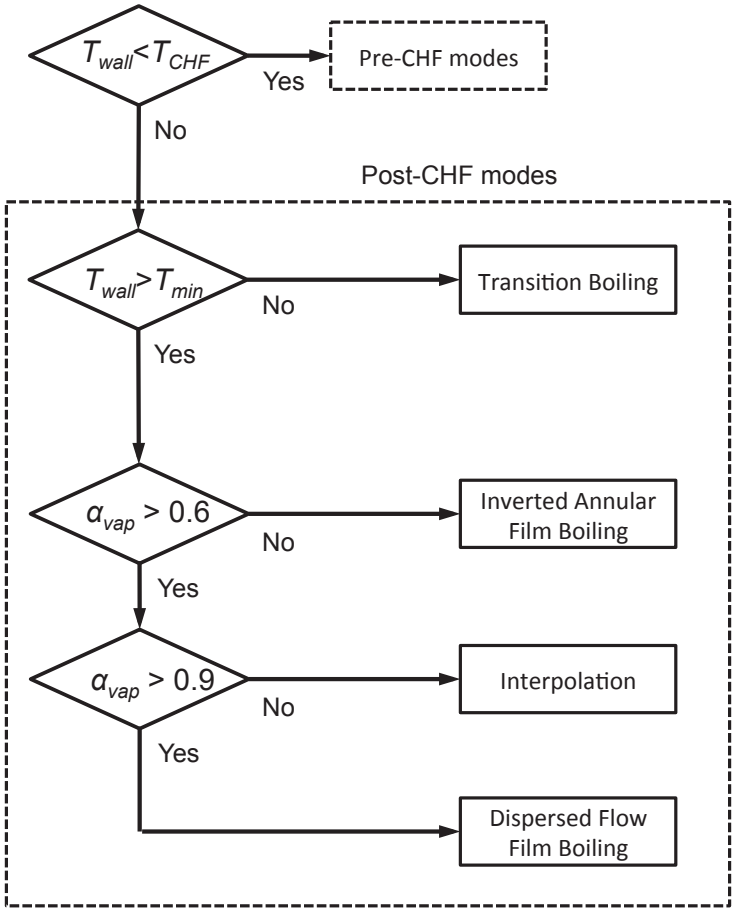

Figure 5. Logic to determine post-CHF wall heat transfer mode following TRACE code [3].

with $\Delta\rho = \rho_{liq} - \rho_{vap}$. Following the TRACE code, the wall-to-liquid radiation heat transfer coefficient is modeled as

$$h_{wall,liq,rad} = \frac{q''_{wall,liq,rad}}{T_{wall} - T_{liq}} = \frac{\sigma_{SB}(T_{wall}^2 + T_{sat}^2)(T_{wall} + T_{sat})}{\frac{1}{\epsilon_{liq}\sqrt{1-\alpha_{vap}}} + \left(\frac{1}{\epsilon_{wall}} - 1\right)}\,, \tag{268}$$

in which σ_{SB} is the Stefan-Boltzmann constant, $5.670 \times 10^{-8}\,\mathrm{Wm^{-2}K^{-4}}$, and ϵ_{liq} and ϵ_{wall} are the liquid and the wall emissivities, respectively. As suggested by the TRACE manual [3], by default, ϵ_{liq} is set to be 0.96, and ϵ_{wall} is set to be 0.7. Finally, the total wall to fluid heat transfer coefficient is

$$h_{wall,liq} = h_{wall,liq,\Gamma} + h_{wall,liq,rad}\,. \tag{269}$$

For wall-to-vapor heat transfer coefficient, following the TRACE manual, a simple model is used:

$$h_{wall,liq} = 2\frac{k_{vap}}{\delta}\,. \tag{270}$$

6.2.2 Dispersed Flow Film Boiling

As in the TRACE code [3], under post-CHF conditions, dispersed flow film boiling is assumed to take place for void fraction greater than 0.9. For dispersed flow film boiling condition, heat transfer between the wall and the two phases is modeled in three components:

$$q''_{wall} = q''_{wall,liq,rad} + q''_{wall,vap,conv} + q''_{wall,vap,rad}\,, \tag{271}$$

in which the three terms on the right hand side are the following, respectively: wall-to-liquid-phase radiation heat flux, wall-to-vapor-phase convective heat flux, and wall-to-vapor-phase radiation heat flux.

6.2.2.1 Wall-to-Vapor-Phase Convective Heat Transfer

For dispersed flow film boiling, wall-to-vapor-phase convective heat transfer is modeled with the single-phase wall-to-vapor heat transfer with a two-phase enhancement factor:

$$q''_{wall,vap,conv} = \frac{k_{vap}}{D_h}\mathrm{Nu}_{wall,vap,conv}\Psi_{2\Phi}(T_{wall} - T_{vap})\,, \tag{272}$$

in which $\mathrm{Nu}_{wall,vap,conv}$ is the single-phase wall-to-vapor convective heat transfer Nusselt number, and $\Psi_{2\Phi}$ is the two-phase enhancement factor. The single-phase wall-to-vapor convective heat transfer is similar to that of single-phase liquid wall heat transfer with

several modifications. Following the TRACE code [3], the Nusselt number is taken as the larger one between a laminar flow value and a turbulent flow value:

$$\mathrm{Nu}_{wall,vap,conv} = \max(\mathrm{Nu}_{lam}, \mathrm{Nu}_{turb}) \,. \tag{273}$$

The TRACE code [3] suggests that a superposition method to be used for the laminar flow value:

$$\mathrm{Nu}_{lam} = \left(\mathrm{Nu}^3_{lam,FC} + \mathrm{Nu}^3_{lam,NC}\right)^{1/3} \,, \tag{274}$$

in which the subscripts FC and NC stand for forced convection and natural convection, respectively.

For natural circulation condition, the laminar flow Nusselt number is modeled as

$$\mathrm{Nu}_{lam,NC} = 0.13 \left[\frac{g\beta_{vap}(T_{wall} - T_{vap})D_h^3}{\nu^2_{vap}} \underset{vap}{\mathrm{Pr}}\right]^{1/3} \,. \tag{275}$$

For forced convection condition, the laminar flow Nusselt number is first calculated based on its geometry, and then corrected with a logarithmic ramp-up factor:

$$Nu_{lam,FC} = wf_{FC} Nu^{'}_{lam,FC} \,, \tag{276}$$

in which wf_{FC} is the ramp-up factor, defined as

$$wf_{FC} = \frac{2 - \log_{10}(\mathrm{Ri})}{2} \,, \tag{277}$$

with $\mathrm{Ri} = \mathrm{Gr}_D/\mathrm{Re}^2_D$ being the Richardson number, and

$$\mathrm{Gr}_D = \frac{g\beta_{vap}(T_{wall} - T_{vap})D_h^3}{\nu^2_{vap}} \,, \tag{278}$$

$$\mathrm{Re}_D = \frac{\rho_{vap} u_{vap} D_h}{\mu_{vap}} \tag{279}$$

The Richardson number is limited to be in between 1 and 100. The geometry-based laminar flow Nusselt number, $\mathrm{Nu}^{'}_{lam,FC}$, is given as a constant, 4.36, for tube geometry. For rod bundle geometry, the same correlations used in single-phase liquid flow conditions are used, i.e., Equation (237).

For turbulent flow of forced convection condition, the Nusselt number, Nu_{turb}, is calculated in a multi-step manner.

$$\mathrm{Nu}_{turb} = \mathrm{Nu}^{'}_{turb} f_{wall} f_{entr} \,, \tag{280}$$

in which Nu'_{turb} is the geometry-based turbulence flow Nusselt number. For tube geometry, the Gnielinski correlation, Equation (227), is used, and for rod bundle geometry, the El-Genk turbulence correlation, Equation (241), is used. The wall temperature correction factor, f_{wall}, is defined as

$$f_{wall} = \left(\frac{T_{wall}}{T_{vap}}\right)^{n} , \tag{281}$$

with

$$n = -\left[\log_{10}\left(\frac{T_{wall}}{T_{vap}}\right)\right]^{1/4} + 0.3 . \tag{282}$$

For the condition that $T_{wall} < T_{vap}$, n is set to be -0.36. The entrance effect is taken into consideration with the entrance correction factor, f_{entr}, that is defined as

$$f_{entr} = 1 + \frac{2.4254}{(L/D_h)^{0.676}} , \tag{283}$$

in which L is the distance to the entrance, and the value of L/D_h is limited to be greater than 3.

Following the TRACE code [3], the two-phase enhancement factor, $\Psi_{2\Phi}$, is modeled as

$$\Psi_{2\Phi} = \left[1 + 25\frac{(1-\alpha_{vap})\mathrm{Gr}_{2\Phi}}{\mathrm{Re}_{vap}^2}\right]^{1/2} , \tag{284}$$

with

$$\mathrm{Gr}_{2\Phi} = \frac{\rho_{vap} g \Delta\rho D_h^3}{\mu_{vap}^2} , \tag{285}$$

with $\Delta\rho = \rho_{liq} - \rho_{vap}$, and

$$\mathrm{Re}_{vap} = \frac{\rho_{vap} u_{vap} D_h}{\mu_{vap}} . \tag{286}$$

The value of the two-phase enhancement factor is limited to be smaller than 5.

6.2.2.2 Wall-to-Liquid/Vapor-Phase Radiation Heat Transfer

Following the TRACE code, the wall-to-liquid/vapor-phase radiation heat transfers are modeled as

$$q''_{wall,liq,rad} = F_{wall,liq}\sigma_{SB}(T_{wall}^4 - T_{liq}^4) , \tag{287}$$

and

$$q''_{wall,vap,rad} = F_{wall,vap}\sigma_{SB}(T_{wall}^4 - T_{vap}^4) , \tag{288}$$

where σ_{SB} is the Stefan-Boltzmann constant, and $F_{wall,liq}$ and $F_{wall,vap}$ are the gray body factors:

$$F_{wall,liq} = \frac{1}{R_2\left(1 + \frac{R_3}{R_1} + \frac{R_3}{R_2}\right)}\,, \tag{289}$$

and

$$F_{wall,vap} = \frac{1}{R_1\left(1 + \frac{R_3}{R_1} + \frac{R_3}{R_2}\right)}\,, \tag{290}$$

where

$$R_1 = \frac{1 - \epsilon_{vap}}{\epsilon_{vap}(1 - \epsilon_{vap}\epsilon_{liq})}\,, \tag{291}$$

$$R_2 = \frac{1 - \epsilon_{liq}}{\epsilon_{liq}(1 - \epsilon_{vap}\epsilon_{liq})}\,, \tag{292}$$

and

$$R_3 = \frac{1}{1 - \epsilon_{vap}\epsilon_{liq}} + \frac{1 - \epsilon_{wall}}{\epsilon_{wall}}\,. \tag{293}$$

For emissivity of the wall, ϵ_{wall}, the same constant value, 0.7, is used. For emissivities of the liquid phase and the vapor phase, the formula used in the TRACE code [5] is used:

$$\epsilon_{liq} = 1 - exp\left[-1.11\frac{\alpha_{liq}}{d_{drop}}L_{beam}\right]\,, \tag{294}$$

and

$$\epsilon_{vap} = \frac{\sum_{i=1}^{6}\eta_i}{1000\sigma_{SB}T_{vap}^4}\,, \tag{295}$$

with d_{drop} as the droplet size, given by Equation (118), and

$$\eta_i = c_1\frac{w_{avg,i}^3}{\exp(c_2 w_{avg}/T_{vap}) - 1}\cdot\{1 - \exp\left[-\min(100, k_i u)\right]\}\cdot dw_i\,. \tag{296}$$

The wave number difference, dw_i, and average wave number, w_{avg}, are given as

$$dw_i = w_{max,i} - w_{min,i}\,, \tag{297}$$

and

$$w_{avg} = \frac{w_{max,i} + w_{min,i}}{2}\,, \tag{298}$$

with

$$w_{min,1-6} = \{195.5, 1283.0, 3399.0, 5043.0, 6942.0, 8468.0\}\,, \tag{299}$$

and

$$w_{max,1-6} = \{804.5, 1892.0, 4008.0, 5652.0, 7551.0, 9077.0\}\,. \tag{300}$$

Parameter, k_i, is given as

$$k_i = \frac{300\alpha_i}{T_{vap}}\,, \tag{301}$$

in which α_i is the absorption coefficient, and

$$\alpha_{1-6} = \{0.0959, 0.2874, 0.2069, 0.0166, 0.0136, 0.00053\}\ . \tag{302}$$

The parameter u is given as

$$u = 9.869 \times 10^{-4} p_{vap} L_{beam}\,, \tag{303}$$

and the radiation path-length in steam, L_{beam}, is given as

$$L_{beam} = 0.9 D_h\,. \tag{304}$$

The two constants are given as $c_1 = 3.747 \times 10^{-5}$ and $c_2 = 1.4394$. Some limitations are applied to the values of the liquid phase and vapor phase emissivities. If the radiation path-length in steam is smaller than 10^{-6} m, the values of ϵ_{vap} and ϵ_{liq} are both set to be 0. If liquid phase volume fraction is smaller than 10^{-5}, the value of ϵ_{liq} is set to be 0.

6.2.2.3 Summary

The following equations summarize the two-phase wall heat transfer coefficients for dispersed flow film boiling conditions:

$$h_{wall,liq} = \frac{q''_{wall,liq,rad}}{T_{wall} - T_{liq}}\,, \tag{305}$$

and

$$h_{wall,vap} = \frac{q''_{wall,vap,conv} + q''_{wall,vap,rad}}{T_{wall} - T_{vap}}\,, \tag{306}$$

with $q''_{wall,liq,rad}$ given by Equation (287), $q''_{wall,vap,conv}$ given by Equation (272), and $q''_{wall,vap,rad}$ given by Equation (288).

6.2.3 Inverted Slug Film Boiling

Under post-CHF condition, when the void fraction is between 0.6 and 0.9, wall boiling heat transfer mode is inverted slug film boiling, which is modeled as a transition region between the inverted annular film boiling and the dispersed flow boiling boiling regions. Following the TRACE manual [3], a linear interpolation is used for each phase k:

$$h_{wall,k} = wf\, h_{wall,k,IAFB} + (1 - wf) h_{wall,k,DFFB}\,, \tag{307}$$

in which the subscripts $IAFB$ and $DFFB$ stand for inverted annular film boiling and dispersed flow film boiling conditions, respectively. The weighting factor is defined as

$$wf = x(2 - x)\,, \tag{308}$$

with

$$x = \frac{0.9 - \alpha_{vap}}{0.9 - 0.6}\,. \tag{309}$$

6.2.4 Transition Boiling

Under post-CHF conditions, when the wall temperature is smaller than the minimum film boiling temperature, T_{min}, the wall boiling heat transfer mode is given as the transition boiling. The minimum film boiling temperature, T_{min}, is given as a function of the liquid phase pressure:

$$T_{min,low}(p_{liq}) = T_{min,sat} - \frac{x \cdot 10^4}{2.82 + 1.22 \times 10^{-6} p_{liq}} \tag{310}$$

for pressure smaller than 9 MPa, and

$$T_{min,high}(p_{liq}) = \left[T_{min,low}(p_{liq} = 9 \times 10^6) - T_{sat}\right] \frac{p_{crit} - p_{liq}}{p_{crit} - 9 \times 10^6} + T_{sat} \tag{311}$$

for pressure greater than 9 MPa. The static flow quality is given by

$$x = \frac{\bar{h} - h_{liq,sat}}{h_{vap} - h_{liq,sat}}\,, \tag{312}$$

with

$$\bar{h} = \frac{\alpha_{liq}\rho_{liq}h_{liq} + \alpha_{vap}\rho_{vap}h_{vap}}{\alpha_{liq}\rho_{liq} + \alpha_{vap}\rho_{vap}}\,. \tag{313}$$

The Groeneveld-Stewart correlation for saturated water is given by

$$T_{min,sat} = 557.85 + 44.1(p_{liq} \cdot 10^{-6}) - 3.72(p_{liq} \cdot 10^{-6})^2\,. \tag{314}$$

The wall-to-fluids heat transfer coefficients are then given as

$$h_{wall,liq} = h_{wall,liq,TB} + (1 - wf_{TB})h_{wall,liq,FB}\,, \tag{315}$$

and

$$h_{wall,vap} = (1 - wf_{TB})h_{wall,vap,FB}\,, \tag{316}$$

with

$$h_{wall,liq,TB} = \frac{wf_{TB}q''_{CHF}}{T_{wall} - T_{liq}}\,. \tag{317}$$

The two heat transfer coefficients, $h_{wall,liq,FB}$ and $h_{wall,vap,FB}$ are calculated from the film boiling heat transfer correlations. The weighting function, wf_{TB}, is modeled as

$$wf_{TB} = \sqrt{1-\alpha_{vap}} \left(\frac{T_{wall} - T_{min}}{T_{CHF} - T_{min}} \right)^2 , \tag{318}$$

in which T_{min} is given by Equation (310) or (311), depending on pressure, and T_{CHF} is the wall temperature when CHF occurs. Similar to the TRACE code [3], an iterative method is implemented to solve for T_{CHF} from

$$q''_{NB}(T_{CHF}) = q''_{CHF} , \tag{319}$$

in which q''_{NB} is calculated from Equation (258), and q''_{CHF} is given by the 1995 AECL-IPPE CHF table as a function of pressure, mass flux, and flow quality:

$$q''_{CHF} = f(p, G, x) . \tag{320}$$

The details on the 1995 AECL-IPPE CHF table are not given in this report, which can be found in the TRACE manual [3], or its original documentation [6].

References

[1] D. Gaston, C. Newman, G. Hansen, and D. Lebrun-Grandié, "MOOSE: A parallel computational framework for coupled systems of nonlinear equations," *Nuclear Engineering and Design*, vol. 239, pp. 1768–1778, Oct. 2009. http://dx.doi.org/10.1016/j.nucengdes.2009.05.021.

[2] R. L. Moore, S. M. Sloan, R. R. Schultz, and G. E. Wilson, "RELAP5/MOD3 Code Manual, Volume 1: Code Structure, System Models, and Solution Methods," Tech. Rep. NUREG/CR-5335, INEL-95/0174, Idaho National Engineering Laboratory, June 1995. http://pbadupws.nrc.gov/docs/ML1103/ML110380259.pdf.

[3] US NRC, "TRACE V5. 0 Theory Manual, Field Equations, Solution Methods, and Physical Models," tech. rep., US NRC. draft.

[4] R. A. Berry, L. Zou, H. Zhao, H. Zhang, J. W. Peterson, R. C. Martineau, S. Y. Kadioglu, and D. Andrs, "RELAP-7 Theory Manual," Tech. Rep. INL/EXT-14-31366 (Revision 2), Idaho National Laboratory, 2014.

[5] Idaho National Laboratory. Communication between INL and U.S. NRC, 2016.

[6] D. C. Groeneveld, et. al., "The 1995 look-up table for critical heat flux in tubes," *Nuclear Engineering and Design*, vol. 163, pp. 1–23, 1996.


INL
Idaho National Laboratory